



1 Cost Effective Off-Grid Automatic Precipitation Samplers for 2 Pollutant and Biogeochemical Atmospheric Deposition

3

4 Alessia A. Colussi¹, Daniel Persaud¹, Melodie Lao¹, Bryan K. Place^{2,‡}, Rachel F.
5 Hems^{2,§}, Susan E. Ziegler³, Kate A. Edwards^{4,‡}, Cora J. Young^{1,2}, and Trevor C.
6 VandenBoer^{1,3}

7

8

9 ¹ Department of Chemistry, York University, Toronto, ON

10 ² Department of Chemistry, Memorial University, St. John's, NL

11 ³ Department of Earth Science, Memorial University, St. John's, NL

12 ⁴ Canadian Forest Service, Natural Resources Canada, Corner Brook, NL

13

14 [‡] Now at: SciGlob Instruments & Services LLC, Columbia, MD, USA

15 [§] Now at: Department of Chemistry and Biochemistry, Oberlin College and Conservatory, OH, USA

16 [†] Now at: Climate Change Impacts and Adaptation Division, Lands and Minerals Sector, Natural Resources Canada, Ottawa, ON

17

18 **Correspondence:** Trevor VandenBoer (tvandenb@yorku.ca)

19

20

21

22 Abstract

23 An important transport process for particles and gases from the atmosphere to aquatic and
24 terrestrial environments is through dry and wet deposition. An open-source, modular, off-grid, and
25 affordable instrument that can automatically collect wet deposition samples allows for more
26 extensive deployment of deposition samplers in fieldwork and would enable more comprehensive
27 monitoring of remote locations. Precipitation events selectively sampled using a conductivity
28 sensor powered by a battery-based supply are central to off-grid capabilities. The prevalence of
29 conductive precipitation, initially containing high solute levels and progressing through trace level
30 concentrations to ultrapure water in full atmospheric washout, depends on the sampling location
31 but is ubiquitous. This property is exploited here to trigger an electric motor via limit switches to
32 open and close a lid resting over a funnel opening. The motors are operated via a custom-built and
33 modular digital logic control board, which have low energy demands. All components, their design
34 and rationale, and assembly are provided for community use. The modularity of the control board
35 allows operation of up to six independent wet deposition units, such that replicate measurements



36 (e.g., canopy throughfall) or different collection materials for various targeted pollutants can be
37 implemented as necessary.

38 We demonstrate that these platforms are capable of continuous operation off-grid for integrated
39 monthly and bimonthly collections performed across the Newfoundland and Labrador Boreal
40 Ecosystem Latitudinal Transect (47° to 53° N) during the growing seasons of 2015 and 2016.
41 System performance was assessed through measured power consumption from 115 volts of
42 alternating current (VAC; grid power) or 12 volts of direct current from battery supplies during
43 operation under both standby (40 or 230 mA, respectively) and in-use (78 or 300 mA, respectively)
44 conditions. In the field, one set of triplicate samplers was deployed in the open to collect incident
45 precipitation (open fall) while another set was deployed under the experimental forest canopy
46 (throughfall). The proof-of-concept systems were validated with basic measurements of rainwater
47 chemistry including: i) pH ranging from 4.14 to 5.71 in incident open fall rainwater; ii)
48 conductivity ranging from 21 to 166 $\mu\text{S}/\text{cm}$; and iii) dissolved organic carbon (DOC)
49 concentrations in open fall and canopy throughfall of 16 ± 10 mg/L and 22 ± 12 mg/L, respectively;
50 with incident fluxes spanning 600 to 4200 $\text{mg C m}^{-2} \text{ a}^{-1}$ across the transect. Ultimately, this
51 demonstrates that the customized precipitation sampling design of this new platform enables more
52 universal accessibility of deposition samples to the atmospheric observation community – for
53 example, those who have made community calls for targeting biogeochemical budgets and/or
54 contaminants of emerging concern in sensitive and remote regions.

55

56 **1.0 Introduction**

57 Atmospheric deposition is the central loss process for particles and gases to terrestrial and
58 aquatic surfaces (Pacyna, 2008). Particles and gases can be deposited by both dry and wet
59 deposition processes. Dry deposition is facilitated by the direct interaction of gases and particles
60 with boundary layer surfaces such as water, vegetation, and/or soil, while wet deposition involves
61 in-cloud scavenging and below-cloud interception of gases and aerosols by, e.g., rain droplets and
62 snow crystals (Fowler, 1980; Lovett and Kinsman, 1990). Dry and wet deposition are global
63 processes coupled to regional synoptic scale conditions, but their relative importance depends on
64 local sources and global transport of atmospheric analytes of interest. Dry deposition consists of a
65 variety of mechanisms for particles and gases, with fine mode particles (compared to ultrafine and
66 coarse mode particles) and their chemical constituents being more likely to undergo atmospheric



67 long-range transport before eventually being deposited (Farmer et al., 2021). Wet deposition
68 occurs when such long-lived atmospheric particles and gases are included and/or scavenged into
69 cloud water and transported to the surface of the Earth in precipitation (e.g., snow and rain). With
70 the size and number of droplets in the atmosphere largely controlling the rate, wet deposition
71 depends on a variety of meteorological factors affecting precipitation, such as the size distribution
72 and concentration of ice and droplet nucleating particles, as well as the solubility, concentration,
73 and reactivity of gases (Lovett, 1994).

74 Ultimately, deposition plays an important role in pollutant distribution and biogeochemical
75 cycling of major nutrients, including long-studied nitrogen and sulfur in acid rain, alongside those
76 with increasing recognition of importance such as dissolved organic carbon (DOC) (Vet et al.,
77 2014; Safieddine and Heald, 2017). If high amounts of atmospheric pollutants or nutrient-bearing
78 compounds are deposited at an environmental interface, this could result in these compounds
79 contaminating the receptor site or exceeding their critical loads for organism or ecosystem
80 function, respectively (Meteorological Service of Canada, 2005; Clark et al., 2018; United States
81 Environmental Protection Agency, 2020). For example, the deposition of nitrogenous compounds
82 to ecosystems can be both desirable or undesirable (Zhu et al., 2015; Kanakidou et al., 2016;
83 Midolo et al., 2019). Although nitrogen deposition could be an additional source of nutrients to
84 plants, in excess it can result in eutrophication and oxygen deficiency in waterbodies due to algal
85 blooms (Pacyna, 2008). Not all atmospheric trace gases can be removed effectively via
86 precipitation, such as sulfur dioxide (SO₂) and nitrogen oxides (NO_x). When these are emitted to
87 the troposphere, they are instead transformed into acids which are readily incorporated into cloud
88 droplets. The nitric and sulfuric acid products are then deposited as environmentally harmful acid
89 rain. These same two classes of acid precursors are released by natural processes, but
90 anthropogenic processes (e.g., the burning of fossil fuels) have been long-established to drive past
91 precipitation acidity (Mohnen, 1988) alongside the subsequent policies enacted to mitigate them.

92 Recognizing the significance of atmospheric trace chemical deposition has led to the
93 establishment of monitoring networks aiming to provide critical data on their spatial and temporal
94 patterns of wet and dry deposition. Long-term wet deposition monitoring networks, like the
95 Canadian Air and Precipitation Monitoring Network (CAPMoN) and the National Atmospheric
96 Deposition Program (NADP), have enhanced scientific knowledge of temporal and spatial
97 deposition. As a result, this has allowed for the estimation of regional and continental deposition



98 rates of species regulated by national or international policies (Lovett, 1994). Data from these
99 networks have been critical to understanding the efficacy of policy to reduce environmental issues
100 like acid rain (Likens and Butler, 2020). In addition to implementing deposition networks, the
101 international community has created protocols (e.g., the Oslo and Geneva protocols) which have
102 achieved an 80% decrease in both North American and European SO₂ emissions since 1980
103 (Grennfelt et al., 2020). However, reductions in acid deposition have had unexpected slow
104 recovery in ecosystems leaving them sensitized – indicating a need for continued deposition
105 monitoring (Stoddard et al., 1999; Kuylentierna et al., 2001).

106 While bulk deposition collection (i.e., a collection bucket or jug fitted with a funnel open
107 at all times; Hall, 1985) is both simple and economically feasible, this sampling method is subject
108 to bias through collection of inputs other than atmospheric deposition (e.g., bird droppings, insects,
109 plant debris). As a result, bulk collectors can overestimate total deposition and underestimate wet
110 deposition in a variety of locations (Lindberg et al., 1986; Richter and Lindberg, 1988; Stedman
111 et al., 1990). Although it is a more costly and time intensive method when compared to bulk
112 deposition collection, the major appeal of measuring isolated wet deposition is that it can be
113 conducted so long as one has a container made of a suitable material for the target analytes and is
114 able to time its deployment and collection to isolate the wet deposition event. Further innovation
115 can reduce bias and improve the preservation of samples, such as the use of sensors to automate
116 isolation of collected precipitation or the addition of polymeric mesh barriers to reduce debris input
117 in windy environments (Lovett, 1994) - yet commercial solutions often come at a substantial
118 expense.

119 Modern emerging issues that require the continuation of existing deposition measurements
120 or expansion of observation programs revolve around identifying and quantifying compound
121 classes of concern, such as persistent organic pollutants (POPs). This group of compounds are
122 characterized by their persistence within the environment and organisms, a high tendency to
123 bioaccumulate, as well as an ability to exert toxic effects – with various POPs being classified as
124 carcinogenic (Safe, 2003; Van den Berg et al., 2006). As a result, atmospheric deposition is an
125 important means by which POPs, or their precursors, are transported from an emission source back
126 to surface environments (Gregor and Gummer, 1989; Fingler et al., 1994; Pickard et al., 2018).
127 The deposition of POPs (e.g., polybrominated diphenyl ethers, polychlorinated biphenyls,
128 polycyclic aromatic hydrocarbons, etc.) can be monitored using suitable collectors made of amber-



129 coloured glass or stainless steel (Fingler et al., 1994; Amodio et al., 2014). For example, on grid
130 bulk collectors and wet-only collectors, with lids triggered by detected conductive precipitation,
131 have been used to isolate the relative role of dry and wet deposition processes (Pekey et al., 2007).

132 When targeting biogeochemically relevant species in deposition collectors, additional
133 standard practices have been developed to improve the representativeness of sample composition.
134 First, an appropriate monitoring site must be selected. Three categories of siting criteria,
135 established by organizations such as CAPMoN and the NADP, are of particular importance: (i)
136 site representativeness and physical characteristics, (ii) distance from potential pollution sources,
137 and (iii) operational requirements (Canadian Air and Precipitation Monitoring Network, 1985;
138 National Atmospheric Deposition Program, 2009). This means that each site must be a location
139 that receives precipitation representative of the hydrologic area; is ideally not within 500 m of
140 local pollution sources, such as wood-burning stoves, garbage dumps, and vehicle parking lots;
141 and is accessible for daily collections, maintenance, and be serviced by reliable 115 VAC electrical
142 power (Canadian Air and Precipitation Monitoring Network, 1985; National Atmospheric
143 Deposition Program, 2009). Despite these guidelines, there are many reasonable scenarios in
144 which these siting conditions cannot be met. As an example, remote sample collections are often
145 required for global assessments on persistent contaminants or nutrients of biogeochemical
146 importance. Remote locations, however, can result in sampling sites with no power provision,
147 infrequent sample collection, and/or the infrastructure-bearing location itself is a source of the
148 targeted pollutants. As a result, innovation in collection strategies such as time-integrated off-grid
149 sampling, with modularity in the deployment of replicates, as well as materials for quantitative
150 collection of environmental targets, is still needed to expand and/or modify networks to meet future
151 monitoring and policy needs.

152 The lack of organic nitrogen (ON) measurements within universally established sampling
153 and measurement procedures serves as a general example of the substantial knowledge gaps that
154 may result when translating limited data sets to the wider global picture. This includes incomplete
155 speciation and quantification across precipitation, aerosol, and gas phases. Monitoring systems
156 that support U.S. deposition assessments (e.g., the NADP) only characterize the inorganic fraction
157 of wet deposition. This results in an incomplete assessment of organic compounds, including
158 several atmospheric groups that have important environmental effects, such as the above-
159 mentioned POPs, reactive nitrogen (N_r), and reactive organic carbon (ROC). Contributions to total



160 N_r by ON compounds in precipitation within the U.S. have been estimated to be between 3% to
161 33% (Benedict et al., 2013; Chen et al., 2018), with a demonstrated abundance of unexpected
162 organic compounds by high resolution mass spectrometry (Altieri et al., 2009, 2012; Ditto et al.,
163 2020). There is a clear and substantial need to improve knowledge of the N_r nutrient pool, amongst
164 other compound classes, to correctly estimate the magnitude of exchange between the atmosphere
165 and terrestrial and/or aquatic environments.

166 In biogeochemical cycles, improvement of constraints in atmospheric carbon linkages to
167 terrestrial and aquatic processes are also critical to correctly assess climate feedbacks and reduce
168 uncertainty in Earth system models. Measurement of atmospheric DOC transport to surfaces has
169 been limited and impedes landscape scale carbon balance from being obtained (Casas-Ruiz et al.,
170 2023). The pool of compounds from which DOC is derived in the atmosphere has also been limited
171 and is only recently seeing an increase in research intensity. Reactive organic carbon, defined as
172 the sum of nonmethane organic gases and primary and secondary organic aerosols (Safieddine and
173 Heald, 2017), is an important driver of oxidative chemistry within the atmosphere. The major
174 removal mechanism of water-soluble organic compounds produced through oxidation from the
175 atmosphere is by dry deposition of particle-bound pollutants and scavenging by rainfall (Jurado et
176 al., 2004, 2005). When ROC is scavenged by dry deposition or rainfall, it becomes DOC and enters
177 terrestrial and aquatic systems. This concept has generated increasing attention around the controls
178 on and composition of DOC in deposition samples. The primary interest is in getting mass closure
179 on atmospheric ROC. Deposition measurements of ROC compounds are also needed since they
180 play a crucial role in the formation of a plethora of secondary species: ozone (O_3), particulate
181 matter, and carbon dioxide (CO_2) (Safieddine and Heald, 2017; Heald and Kroll, 2020).

182 There are several evolving drivers around studying atmospheric ROC; for example, light-
183 absorbing organic carbon that accumulates in the atmosphere can affect global radiative balance
184 and can change over time through photochemical transformations in the condensed phase (Saleh,
185 2020; Wang et al., 2021; Washenfelder et al., 2022; Geroge, 2023). Reactive organic carbon can
186 also influence cloud formation and its contribution to precipitation acidity (Avery et al., 2006;
187 Ramanathan and Carmichael, 2008). Measurements of speciated ROC are difficult due to the
188 chemical complexity of emitted compounds and oxidation products (Heald and Kroll, 2020). To
189 circumvent this, monitoring and quantifying DOC can be used as a proxy to estimate the total ROC
190 in precipitation. However, quantitative measurements of DOC in precipitation samples are sparse



191 due to its relatively low concentration which has been reported between 0.1 to 10 mg C L⁻¹ in
192 incident precipitation (Iavorivska et al., 2016; Safieddine and Heald, 2017). Recently, calls for
193 carbon closure on atmospheric processing of ROC make this measurement of increasing
194 importance (Kroll et al., 2011; Heald et al., 2020; Barber and Kroll, 2021). Similarly, to obtain net
195 landscape or watershed carbon exchange, studies require effective methods for capturing and
196 preserving atmospheric DOC deposition to constrain biogeochemical linkages at global interfaces
197 as outlined above.

198 In this work, we present the design of a custom-built automated array of precipitation
199 samplers that can be operated both on- and off-grid for wet deposition collection. The purpose of
200 these samplers is to enable cost-effective collection of monthly integrated water-soluble
201 conductive atmospheric constituents deposited in remote environments without grid power or
202 routine access. A sensor interfaces with a custom-built motor control board capable of operating
203 up to six independent wet deposition units such that canopy throughfall (TF) and incident
204 precipitation measurements are possible to collect in replicate. The materials used can be easily
205 changed in order to optimize collection of a wide array of target analytes, such as POPs or DOC.
206 We demonstrate that these platforms are capable of continuous operation off-grid for monthly wet
207 deposition collection of precipitation across the Newfoundland and Labrador Boreal Ecosystem
208 Latitudinal Transect (NL-BELT) during snow-free periods in 2015 and 2016. Extremes in system
209 performance were evaluated by testing the power consumption of a sampling array from spring
210 through fall when paired with a solar top-up system, and during snow-free winter conditions using
211 only a battery. The two years of field samples were collected using an array of six collection units,
212 with triplicate collection of both incident precipitation and throughfall from rain passing through
213 a forest canopy. Samples were analyzed in terms of deposition volumes relative to total bulk
214 volumes, to assess the reproducibility of replicate samples, and determine the fraction of
215 conductive rainfall collected from the total volume of precipitation. The captured fraction
216 compared to total volume deposited is used to gain insight into limiting analyte dilution effects
217 and improving deposition method detection limits. Chemical parameters of pH, conductivity, and
218 DOC fluxes were then used to validate this proof-of-concept system. Measurements of pH and
219 conductivity for rainwater are very well-established in the literature and serve as a baseline
220 reference to ensure that the samples collected by the new devices presented in this work are
221 consistent with what is expected in samples from a remote coastal environment, given the selective

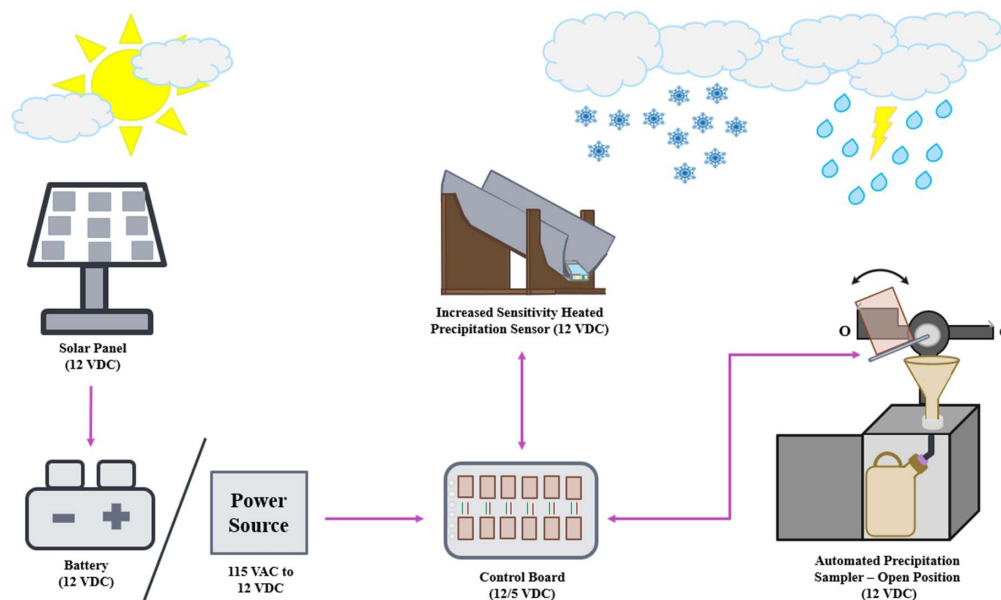


222 sampling strategy. We then move away from these well-established parameters to quantify DOC
223 fluxes to demonstrate the potential of these samplers in application to automated collection of
224 analytes of emerging importance and interest in remote locations spanning our latitudinal transect.
225

226 **2.0 Materials and Methods**

227 **2.1 Precipitation Sampling Array Components**

228 Each automated precipitation sampling setup can be operated as an array, here being used
229 in groups of up to six collection units (Figure 1). A collection unit is a simple opaque doored box.
230 The box protects the sample containers against exposure to direct sunlight and provides a mounting
231 location for the funnel and lid, while also facilitating easy exchange of sample containers. The
232 collection units can be fitted with stabilizing legs that allow them to be bolted to concrete or pinned
233 by retaining rods when on soil. In both cases, this prevents tipping and loss of sample during high
234 winds or wildlife-sampler interactions (e.g., Figures 2 and S1). The collection of precipitation is
235 facilitated by a funnel mounted through the top of the sampling unit. The funnel tip extends into
236 the opening of the sample collection container placed inside. The connection can be sealed to better
237 preserve volatile analytes with tubing that passes through a sealed grommet (P/N 9280K34,
238 McMaster-Carr) to enter the sample collection container and minimize evaporative losses.
239 Precipitation events are sampled selectively by modulating the position of a lid over the funnel
240 with an electric motor. The collection unit motors are operated by a digital control board, which
241 interfaces with a precipitation sensor and requires 12 volts of direct current (VDC) power supplied
242 to this system. Switches detecting the lid position ensure complete opening or closure of the funnel
243 mouth for each collection unit.

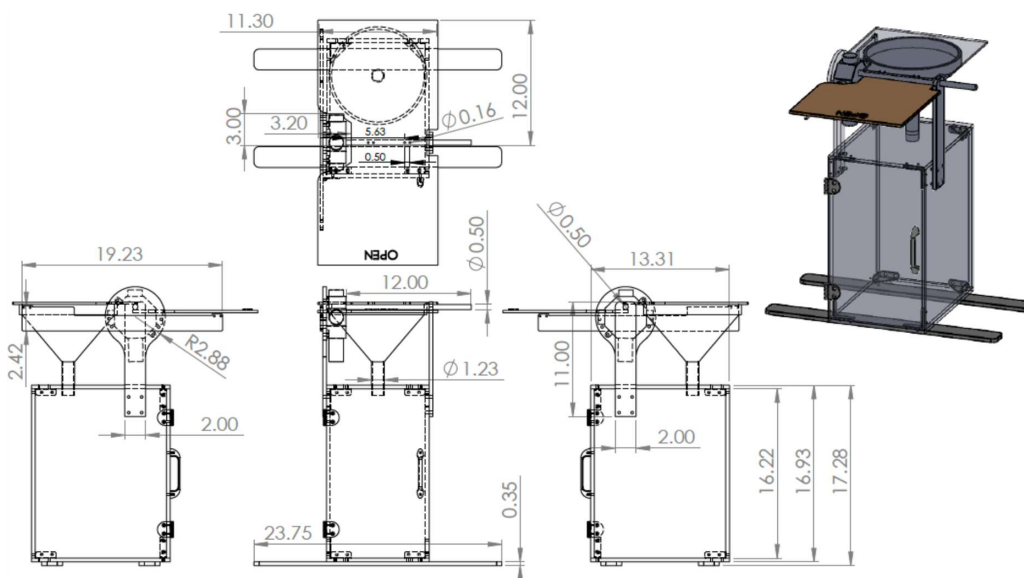


244
245 **Figure 1.** Schematic of custom-built automated precipitation sampling array components for off-
246 grid wet deposition collection. The pink arrows denote the direction of electrical signal and power
247 exchanged between components. The curved black arrow indicates the rotation of a motorized lid
248 to obtain open (O) or closed (C) sampler configurations.
249

250 2.1.1 Collection Units

251 The collection unit materials to date have been made of both 3/8" plywood and black
252 polyacrylate sheeting. The materials have demonstrated high durability on the order of four years
253 under field conditions (Figures S1 and S2). Opaque materials were explicitly selected to minimize
254 photochemical reactions and growth of photosynthetic microorganisms within the sample. The
255 dimensions of the collection unit are detailed in Figure 2. Each can accommodate sample
256 containers up to 20 L in volume for collection in locations with large monthly wet deposition
257 volumes, such as in Newfoundland and Labrador (Table 1).

258



259

260 **Figure 2.** Detailed collection unit schematic with all dimensions provided in inches. Further
261 specifications for the lid dimensions can be found in Figure S3. The shaded 3D rendering depicts
262 both open and closed states for the lid, positioning of legs to secure it to surfaces, placement of
263 corner brackets, and the door handle and hinges.
264

265 The box panels can be joined using hardware inserts (P/N 1556A54 and 1088A31,
266 McMaster-Carr, Aurora, OH), 3D printed corners (Figure S4), or along the box edges with screws
267 if using wood. The door is attached with two hinges (P/N 1549A57, McMaster-Carr) and held
268 closed with a magnetic contact (P/N1674A61; McMaster-Carr) or hooked latch. The electric motor
269 controlling the lid is enclosed in a standard polyvinylchloride electrical junction box, which is
270 attached to a short paddle mounted on one side of the collection unit. Here we used an electric
271 worm-gear motor (12 VDC, 2 rpm; TS-32GZ370-1650; Tsiny Motor Industrial Co., Dong Guan,
272 China) mounted inside the enclosure with matching hex bolts (P/N 91251A146, McMaster-Carr)
273 that passed through the weather-tight cover while the drive shaft protrudes through a 3/8" hole
274 drilled in the cover. The drive shaft has a flat edge to affix the lid rod using a short set screw
275 (Figure S5) that is cemented semi-permanently in place with thread locking compound (P/N
276 91458A112; Loctite Threadlocker Blue 242; McMaster-Carr). The lid rod is 3/8" aluminum
277 machined on one end to allow connection to the motor drive shaft (Figure S5) with four threaded
278 holes along its length to affix the lid (Figure S3). The lid rod passes through a second mounting



279 paddle on the box that keeps the lid level and capable of isolating the funnel from the atmosphere
280 in the absence of precipitation. The lids used here were made of 1/8" Lexan polycarbonate sheet.

281 Selective precipitation sampling is performed using a logic-based assessment of sensor and
282 switch states (defined in Figure S6) by the control board quadNOR gate chip (Fairchild
283 Semiconductor P/N DM74LS02) which activates the H-bridge motor driver chipset (Figure S7).
284 A 12 VDC signal drives the clockwise or counterclockwise rotation of the motor, installed in a
285 suitable port of the junction box, via a cable from the control board, which passes through a
286 weather-tight compression fitting (e.g., Home Depot SKU# 1000116446). The motor rotation
287 signal is interrupted when the lid makes contact with one of two weather-tight limit switches (P/N
288 SW1257-ND; Omron, Digi-Key Electronics, Thief River Falls, MN) mounted on opposite ends of
289 a horizontal armature connected to the vertical motor mounting paddle (Figure 2). The switches
290 controlling the lid location ensure that the funnel is completely open or covered as necessary for
291 precipitation collection. The funnels used in this work are 20 cm in diameter and made from high-
292 density polyethylene (HDPE; Dynalon, P/N 71070-020, VWR International, Mississauga, ON). A
293 7" x 5" piece of filtration mesh (P/N 9265T49, McMaster-Carr) that was tied together as a fitted
294 cone insert with Nylon thread (e.g., fishing line) to prevent large debris entering the sampler
295 containers when used, for example, in the collection of TF precipitation under a forest canopy
296 when accompanying litterfall is also expected. The exit of the funnel directs the collected
297 precipitation into the narrow-mouth opening the container inside the collection unit, such as 20 L
298 HDPE jugs or 10 L HDPE jerricans (Bel-Art Products; P/N 11215-314, VWR International).

299

300 **2.1.2 Heated Precipitation Sensor**

301 The detection of rain modulates the opening and closing of the collection units by an
302 interdigitated resistive sensor (M152; Kemo Electronic GmbH, Geestland, Germany; Figures S6
303 to S8). The rain sensor detects conductive deposition by the completion of a conductive circuit
304 when electrolytes bridge the connection between the interdigitated gold electrodes. The sensor is
305 supplied with 12 VDC from the power system to trigger a relay when precipitation conductance
306 above 1 M Ω ·cm conductivity is detected (determined experimentally, see Sect. S1). An output of
307 12 VDC is sent to the digital control board by the relay when rain is sensed, or 0 VDC in its
308 absence, for signal processing and motor control (Figure S7). To increase the sensitivity of this
309 sensor and to extend the sampling duration when conductive atmospheric constituents are



310 completely washed out of the atmosphere, a sloped tin chute (e.g., Home Depot SKU#
311 1001110514) was added to extend the surface of the rain sensor. The sensor was placed at the end
312 of the chute and sealed in place with caulking to allow water droplets to move easily from the
313 chute onto the sensor.

314 The angle of the chute can be adjusted to control the momentum of collected droplets so
315 that they collect on the sensor surface and only flow off it when the rate of precipitation exceeds
316 the sensor evaporation capability. When soil is available, two bent rods can be used to hold the
317 chute at the optimized angle of 10° (Figure S2). They are inserted into the soil and the chute is
318 affixed to the tops of the rods with zip ties passed through small holes drilled in the sides of the
319 chute, which are subsequently sealed with caulking. When soil is unavailable, for example in urban
320 environments, we have created a mounting frame to hold the chute at the optimized angle of 10°
321 (Figure S8). When precipitation is detected the sensor surface draws current up to 1.0 ampere (A)
322 into a heater to actively evaporate water from its surface so that it accurately detects the active
323 period of rain events. The heated sensor has undergone preliminary field tests and is also capable
324 of detecting ice and snow, provided they contain electrolytes.

325

326 **2.1.3 Power Supply Systems**

327 Power for this system can be supplied from a battery at 12 VDC or using a 115 VAC to 12
328 VDC transformer power supply (P/N 285-1818-ND; TDK-Lambda Americas, Digi-Key
329 Electronics). Depending on the duration of sampling and the time of year, the battery capacity can
330 be changed to suit power needs (Sect. 3.2.2). To provide sufficient power density in this study,
331 over one to two month-long collection periods, the battery capacity was carefully matched; with
332 top-up options implemented when prolonged or high-frequency precipitation was expected.
333 Absorbent glass mat (AGM) marine deep cycle batteries can withstand discharge events down to
334 less than 60 % capacity and are robust under nearly all environmentally relevant temperatures (\leq
335 -20°C to 40°C). Additionally, these batteries interface easily with solar charging options as they
336 are able to accept high current input. Monthly collections in Newfoundland were powered with 76
337 amp-hour (Ah) AGM batteries (Motomaster Nautilus; Ultra XD Group 24 High-Performance
338 AGM Deep Cycle Battery, 12 VDC) topped up by a 40 W solar panel interfaced with a charge
339 controller to prevent overcharging (Coleman; Model # 51840, max current of 8 A at 14 VDC).



340 For collections made every second month in Labrador, a 120 Ah battery with the same
341 solar top-up strategy was used to ensure continuous operation. For either remote field deployment,
342 batteries and charge controllers were housed in a Pelican™ case (Model 1440, Ocean Case Co.
343 Ltd., Enfield, NS) fitted with weathertight bulkhead cord grips (P/N 7529K655, McMaster-Carr)
344 through which charging and power cables were passed (Belden, Coleman; S/N 7004608,
345 70875227, Allied Electronics, Inc., Ottawa, ON). Humidity in all weatherproof cases was
346 minimized by exchanging reusable desiccant packs (Ocean Case Co. Ltd.) when depleted batteries
347 were exchanged for fully charged replacements. Solar panels were repositioned monthly to
348 optimize orientation for solar power provision. Using either power source, the control board
349 converts and distributes the 12 VDC to the other components in the precipitation sampling array.
350

351 **2.1.4 Custom Control Board**

352 A custom control board to operate a six-collection unit array was designed based on prior
353 digital logic circuits for standalone collectors (VandenBoer, 2009). The 12 VDC battery or
354 transformer output is supplied directly to the rain sensor and relay, as well as to the motor drivers
355 for lid opening (Figure S9). Each collection unit is controlled independently to ensure lids are fully
356 opened or closed, thereby requiring six replicate motor driver control circuits that respond to their
357 independent switch signals. The remainder of the signaling and digital logic operates on 5 VDC
358 which is produced by on-board voltage regulators (Micro Commercial Co; P/N MC7805CT-BP,
359 Digi-Key Electronics). The lid switches are provided with 0 and 5 VDC to indicate collection unit
360 open or closed status (Omron Electronics; P/N D2FW-G271M(D), Digi-Key Electronics). The
361 signals from the sensor and switches connect to the board through four-conductor cable (Belden;
362 S/N 70003678, Allied Electronics Inc.) passed through weathertight bulkhead cord grips and
363 secured to screw terminals (Figure S9). The sensor and switch signal inputs interface with a quad
364 NOR GATE chipset (Texas Instruments; P/N 296-33594-5-ND, Digi-Key Electronics) to trigger
365 the motor driver (STMicroelectronics; P/N 497-1395-5-ND, Digi-Key Electronics) such that it
366 rotates or remains stationary. The additional resistors, capacitors, and diodes are necessary to
367 maintain stable signaling throughout the printed circuit board (Figure S9, Table S1).

368 The custom control board was housed in a Pelican™ case (1400 NF; Pelican Zone,
369 Mississauga, ON) fitted with cut-to-use foam inserts and a reusable desiccant pack that was also
370 exchanged alongside those for the battery cases. All collection units, sensors, and power supply



371 cables were passed through eight weathertight bulkhead cord grips and fixed to screw terminals
372 on the board. The opposing ends of the cables were fitted with weathertight Bulgin Buccaneer 400
373 or 4000 Series circular cable connectors (Table S2; Allied Electronics, Inc.) to allow easy field
374 installation with mated connectors on the cables originating from each of the previously mentioned
375 array components. Connected cables could then be buried in shallow soil trenches to reduce the
376 attention of gnawing animals, as well as potential entanglement hazards with other wildlife.
377 Precipitation events were logged from the control boards using a HOBO 4-channel analog data
378 logger (UX120-006M; Onset[®], Bourne, MA) that records the sensor, switch, and motor voltages.
379 The fourth channel is reserved to monitor battery or power supply voltages over time (Sect. 3.2).

380

381 **2.2 Power Demand and Management Tests**

382 Power demand was calculated based on the cumulative component requirements prior to
383 the selection of batteries. This was to ensure adequate capacity to collect samples over one to two
384 month-long field deployments and are sufficient for an assumed worst-case scenario of one week
385 of constant rain without solar power charge restoration. Solar panel power production capacity
386 was determined based on the calculated energy required to recharge the battery. As a result, we
387 selected the 40 W panel which could complete charging at 14 VDC with a week of direct sunlight
388 at 8 hours per day. The power demand for a six-sampler array was measured in standby and during
389 operation with a digital power meter (Nashone PM90, Dalang Town, China) in real-time when
390 supplying 12 VDC with a transformer. Contrasting power demand tests were performed under
391 different environmental conditions and power management configurations. The first was
392 performed using the 76 Ah AGM battery with a solar top-up in an urban environment from July
393 through August 2018, while the other was performed using a 103 Ah AGM battery alone from
394 January through February 2019.

395

396 **2.3 Continuous Monthly Collection of Remote Samples at NL-BELT**

397 Four arrays of six automated collection units and total deposition samplers were deployed
398 within one forested experimental field site located in each of the four watershed regions of the NL-
399 BELT between 2015 and 2016 (Table 1, Figure S10). The watersheds span 5.5° latitude from the
400 southernmost site Grand Codroy (GC), through the colocated Pynn's Brook (PB) and Humber
401 River Camp 10 (HR) sites, to Salmon River (SR) as the highest latitude site on the island of



402 Newfoundland. The northernmost forested watershed, Eagle River (ER), is located in southern
 403 Labrador and extensive details characterizing each of the four sites can be found in Ziegler et al.
 404 (2017). All sampling locations are far from anthropogenic pollutant point sources, except for the
 405 ubiquitous presence of marine sea spray from the nearby marine coastlines. The total deposition
 406 samplers were identical to the automatic collection units except that they were not fitted with a
 407 motor arm and lid, so they did not require a source of power. Three of the six automated samplers
 408 were deployed in the open at a distance from the forest stand, equal to or greater than the height
 409 of the trees, in line with CAPMoN and NADP guidelines. The other three automated samplers
 410 were placed under the canopy to collect TF precipitation within the forest sites. These samplers
 411 actively collected wet deposition into integrated monthly (Newfoundland) or two month
 412 (Labrador) samples during snow-free periods (approximately June through November). The arrays
 413 were collected and stored during the winter months while total deposition samplers remained in
 414 field locations year-round. It is also important to note that during the growing season, sample
 415 collections were made at the same time – that is, open fall (OF) and TF deposition were collected
 416 on a single day at each sampling site and within a few days of each other across the transect.
 417 Collected sample volumes were compared between the automated samplers and total deposition
 418 collectors for each collection interval as a check on proper function (i.e., less than or equal volumes
 419 in automated samples).

420 **Table 1.** NL-BELT sampling site details provide locations and identifiers, alongside those from
 421 long-term weather stations operated by Environment and Climate Change Canada (ECCC). Soil
 422 pH was determined from samples collected at the same time as precipitation. Mean annual
 423 temperature was derived from ECCC climate normals. Annual total deposition precipitation
 424 volumes were either measured for the 2015-16 period (ECCC, This Work) or calculated by the
 425 Oak Ridge National Lab DAYMET archive.
 426

Sampling Site	Sampling Site Location	Station (Climate ID)	Station Location	Soil pH ^a	MAT (°C) ^b	Average Annual Precipitation (L)		
						ECCC ^c	DAYMET ^a	This Work
Grand Codroy (GC)	47°50'43.1"N 59°16'16.0"W	Stephenville A (8403801)	48°32'29.00" N 58°33'00" W	3 to 4	5.0 ^c	53.2	58.9	45.6 (+5.17)
Pynn's Brook (PB)	49° 05' 13.20"N 57° 32' 27.60" W	South Brook Pasadena (8403693)	49°01'00" N 57°37'00" W	3 to 4	4.6 ^c	21.4	54.3	38.6 ^a
Salmon River	51°15'21.6"N 56°08'16.8"W	Plum Point (40KE88)	51°04'00" N 56°53'00" W	3 to 4	2.4 ^c	47.1	45.4	32.3



(SR)

Eagle River (ER)	53°33'00.0"N 56°59'13.2"W	Cartwright A (8501100)	53°42'30" N 57°02'06" W	3 to 4	0 ^d	- ^e	56.3	25.8
------------------------	------------------------------	---------------------------	----------------------------	--------	----------------	----------------	------	------

427

428 ^aSoil pH for the organic and mineral soil horizons determined by addition of 400 µL of aqueous 0.5 M CaCl₂ to a 50:50 w/w slurry
429 of dried soil in deionised water.

430 ^bEnvironment Canada: Canadian Climate Normals, 1981 to 2010, https://climate.weather.gc.ca/climate_normals/ (last accessed:
431 14 July 2023).

432 ^cAt least 20 years of measurements.

433 ^dThe World Meteorological Organization's "3 and 5 rule" (i.e., no more than 3 consecutive and no more than 5 total missing for
434 either temperature or precipitation).

435 ^eAnnual precipitation averages determined using ECCC daily precipitation reports.

436 ^fLarge quantity of missing data for this location from January 2015 to December 2016 prevents any reliable estimate.

437 ^gEstimated deposition rates converted to volume using DAYMET (Thornton et al., 1997, 2021, 2022).

438 ^hVolumes merged for 2015 and 2016 at PB and HR.

439

440

441 During each site visit, the slope of the sensor was confirmed to be correct, sample
442 containers were collected and replaced with clean units, the battery and desiccant packs replaced
443 with fully recharged devices, and the entire array confirmed operational. Four of the six sample
444 containers (two each of OF and TF) were biologically sterilized using 1 mL of a saturated aqueous
445 solution of mercuric chloride (HgCl₂) to preserve against biological growth and loss of
446 bioavailable nutrients over the collection periods. Unsterilized sample containers (without HgCl₂)
447 were used for measurements of recalcitrant species and to assess any matrix effects exerted by the
448 preservation technique on target analyte quantitation. Collected sample volumes were measured
449 with a 1000 ± 10 mL graduated cylinder and aliquots were collected for chemical analysis via
450 transfer to precleaned 500- or 1000-mL HDPE containers (Nalgene; VWR International). Samples
451 were stored at 4 °C before returning to the laboratory where they were filtered with a 1000 mL
452 Nalgene vacuum filtration system (P/N ZA-06730-53; ThermoFisher Scientific, Waltham, MA),
453 fitted with 0.45 µm polyethersulfone filters (PES, P/N HPWP 04700, EMD Millipore), to remove
454 suspended solids. Filtered samples were transferred to new clean HDPE containers and stored for
455 up to two months at 4 °C in a cold room until analysis.

456

457 **2.4 Cleaning and Preparation of Sample Containers**

458 All sample collection and storage containers, as well as all sample handling apparatuses,
459 were made of HDPE or polypropylene for the quantitative analysis of target analytes. Prior to use
460 in handling samples, these were all acid-washed in 10 % v/v HCl (P/N BDH7417-1; VWR
461 International) followed by six sequential rinses with distilled water and ten rinses with 18.2



462 $\text{m}\Omega\cdot\text{cm}$ deionised water (DIW; EMD Millipore Corporation, Billerica, MA, USA). Containers
463 were dried by inversion on a clean benchtop protector overnight, or with protection from dust using
464 lint-free lab wipes over container openings when necessary. Field and method blanks were
465 collected through the addition of DIW to cleaned containers, and/or sample handling devices, in
466 order to quantify appropriate method detection limits and to identify any sources of systematic or
467 random contamination.

468

469 **2.5 Measurements of pH and Conductivity**

470 The pH and conductivity of each sample was determined using a ThermoScientific™ Orion
471 Versa Star meter (ORIVSTAR52) interfaced with a pH electrode (Model: 8157BNUMD, Ultra
472 pH/ATC Triode, ROSS) and 4-electrode conductivity cell (Model: 013005MD, DuraProbe,
473 ROSS). Prior to use, the probes were calibrated daily with standard solutions specific for these
474 probes (ThermoScientific™ Orion™ conductivity standard 1413, and pH 4, 7, and 10 buffers) and
475 then stored between analyses according to manufacturer directions. Aliquots of 15 mL of
476 precipitation from archived samples were subsampled into 40 mL polypropylene Falcon tubes.
477 This was followed by immersion of a cleaned electrode for the conductivity measurement,
478 followed by the pH probe measurement to prevent conductivity bias due to potassium chloride
479 migration across the glass frit of the pH probe. Readings were recorded once signals had stabilized.
480

481 **2.6 Measurements of Dissolved Organic Carbon (DOC)**

482 Measurements of DOC were performed by catalytic combustion of samples in a platinum
483 bead-packed quartz furnace at 720 °C to quantitatively produce CO_2 , followed by non-dispersive
484 infrared absorption spectrophotometry using a Shimadzu Total Organic Carbon (model: TOC-V)
485 analyzer and an autosampler (model: ASI-V). Cleaning of materials prior to DOC determination
486 follows the same procedure as for the sample containers. Precipitation aliquots of at least 12 mL
487 were transferred to clean and combusted (500 °C, 5 hours) 40 mL borosilicate glass vials, then
488 capped and stored at 4 °C until analysis. Prior to analysis, vial caps were replaced with cleaned
489 polytetrafluoroethylene-lined septa. Inorganic dissolved carbon (e.g., H_2CO_3) was purged from
490 samples by acidification to pH 2 with HPLC grade H_3PO_4 (20 % v/v) and bubbling with an inert
491 carrier gas. Samples were analyzed in triplicate and quantified using calibrations spanning 0.1 to
492 10 or 10 to 100 ppm (mg C L^{-1}) with potassium hydrogen phthalate (KHP), depending on the



493 relative sample concentration range. Accuracy and precision were assessed using 1 and 10 ppm
494 KHP check standards analyzed every 10 injections, respectively. Calibrations were performed at
495 the beginning of every analysis day.

496

497 **3.0 Results and Discussion**

498 In addition to the general design advantages in the section that follows, we present the
499 results of various physical and chemical parameters to validate this new open source custom-built
500 modular system. The power consumption and snow-free performance testing are used to
501 demonstrate the off-grid capabilities of these samplers, as are the two-year datasets. The lower
502 power requirements are compared to existing commercial samplers and paired with solar top-up
503 to prolong the use and reduce the need to replace batteries on timescales shorter than planned
504 sampling duration (i.e., < 1 month). We then evaluate the automated wet deposition volumes, in
505 which the samplers prevent dilution during atmospheric washout events, compared to total
506 volumes collected from co-located samplers to depict the fractionation by volume as a function of
507 time. We also investigate the advantages of replicates collected across the four watersheds, using
508 deployments of triplicate samplers under field conditions. The ratio of collected TF to OF
509 replicates highlights the ability of these samplers to capture the dynamic nature of precipitation
510 interacting with forest canopies. Simple pH and conductivity measurements are then used as
511 benchmarks to situate the NL-BELT data within the established literature to emphasize the robust
512 operation of the samplers and impact of the selective sampling. Fluxes of DOC are then
513 interrogated across all four sampling sites as we demonstrate the potential of these samplers to
514 make measurements of more complex analyte pools that are of current interest to the atmospheric
515 measurement community.

516

517 **3.1 General Design Advantages**

518 When compared to other precipitation collection apparatuses, the automated precipitation
519 sampler developed in this work has several advantages. Most notable is the ability to collect
520 integrated samples at remote locations by exploiting its off-grid capabilities. Our approach also
521 maximizes the sensitivity of the rain sensor as long as electrolytes remain in the water reaching it.
522 The chute ensures that even if the precipitation contains ultra-trace analyte quantities, they are still
523 collected and quantified for an extended period when high-purity water may be deposited during



524 an atmospheric wash-out event. The chute does this by accumulating water-soluble materials
525 between rain events that require time to be completely washed off and through the release of ions
526 from the material itself, which ages under environmental conditions. As the conductivity of the
527 precipitation falls below the sensor threshold, the added ions from the chute prolong the collection
528 of rain past this time point. In rainfall events where extended atmospheric wash-out occurs, the
529 sampler lids will eventually close – preventing dilution of the sample while maintaining the
530 collection of analytes of interest. In application to trace pollutants, this also reduces
531 methodological sample preparation time as it decreases the extent to which additional handling
532 steps, like solid-phase extraction, are required prior to analytical determinations.

533 The six replicate measurements used in each array provide a means of assessing sampling
534 reproducibility (e.g., canopy TF has expected heterogeneity) and for multiple analyte classes to be
535 targeted. Various analytes, with different chemical properties and/or contamination considerations,
536 can be targeted by changing the materials used for the components that encounter the sample (i.e.,
537 lids, funnels, and sample holding containers). Replicate collection can also allow for selective
538 sample preservation when quantifying deposited chemical species that may be reactive, volatile,
539 or biologically transformed. The modularity of the overall system design also allows the collection
540 units to be dismantled entirely and easily reassembled on-site, minimizing logistical issues and
541 costs for transport to remote regions. Lastly, these collection units are cost-effective. We were able
542 to produce four arrays, each consisting of six collection units, at a fraction of the cost of a single
543 equivalent commercial off-grid automated precipitation sampling unit.

544 With the majority of commercial precipitation samplers requiring a source of electricity,
545 on-grid sample collection necessitates high infrastructure costs and/or samplers being positioned
546 closer than desired to point sources of anthropogenic pollution. As a result, especially in remote
547 locations, site selection becomes heavily restricted and expensive when factoring in all the
548 standard criteria, particularly with respect to the need for an easily accessible power source. Thus,
549 the off-grid capabilities of our samplers lends dexterity to these systems and makes deposition
550 sampling that follows standard siting guidelines, like those of CAPMoN or NADP but without
551 power, more accessible to the global atmospheric research community (Vet et al., 2014). To further
552 highlight and validate their capabilities, a series of fundamental performance parameters were
553 collected and are discussed in detail in the sections that follow.

554



555 3.2 Power Consumption and Performance Testing

556 3.2.1 Power Consumption of Instrumental Setup

557 The simplicity of the automated precipitation samplers allows for low power consumption
558 during operation, which is particularly important for off-grid operation. The motors operating and
559 rain sensor heating during active precipitation are the most energy-intensive elements of the system
560 (Table 2). The integrated contribution of the motor over a month-long sampling period is however
561 negligible compared to other components, since it is operational for short periods of 5 to 10
562 seconds with a current usage of only 38 mA. The continuous need to provide 5 VDC to the digital
563 logic via step-down from 12 VDC is actually the largest power consuming component of the setup
564 in the absence of rain. When the samplers are in the closed position, under rain-free conditions,
565 the power consumption of the entire array is 4.66 Watts (W) and 2.86 W for transformed 115 VAC
566 and battery 12 VDC supplies, respectively. The provision of 12 VDC to the board with a
567 transformer for the 115 VAC application results in greater total power requirements. These values
568 increase to 10.00 W and 5.04 W with the detection of a conductive liquid on the precipitation
569 sensor as it heats the sensor surface to capture the active period of the event. Based on the measured
570 power consumption, a fully charged 103 Ah AGM battery would provide at most 447 hours (or 18
571 days) in standby mode under rain free conditions and 294 hours (or 12 days) if the heated surface
572 of the sensor is in continuous use (Table 2). The lower range limit is unlikely since the sensor only
573 operates for the duration of a rain event, after which the battery is available for solar top-up again.
574 In the fieldwork conducted here, battery life was extended through the addition of 40 W solar
575 panels to the systems. The entire array was confirmed to be operational at the end of monthly (SR,
576 PB, and GC) and two month (ER) integrated sampling periods on a ongoing basis, prior to
577 exchange with a new fully-charged battery, for two years.

578
579
580
581
582
583
584
585



586
 587
 588
 589

Table 2. Measured voltage, current, and power consumption of the rain sensor and circuitry in both the idle and maximally operational state when connected to a 12 VDC battery or transformed 115 VAC. Total power demand was measured for wet and dry sensor scenarios.

Parameters	Rain Sensor		AC Outlet		DC Battery		Total			
	Idle	Active	Idle	Motors	Idle	Motors	Dry	Wet	Dry	Wet
			Board	In-Use	Board	in-Use				
Voltage (V)	12 DC	12 DC	114 AC	110 AC	12 DC	12 DC	-	-	-	-
Current (A)	0.008	0.120	0.040	0.078	0.230	0.300	-	-	-	-
Power (W)	0.10	1.44	4.56	8.58	2.76	3.60	4.66	10.00	2.86	5.04

593
 594
 595
 596
 597
 598
 599
 600
 601
 602
 603
 604
 605
 606
 607

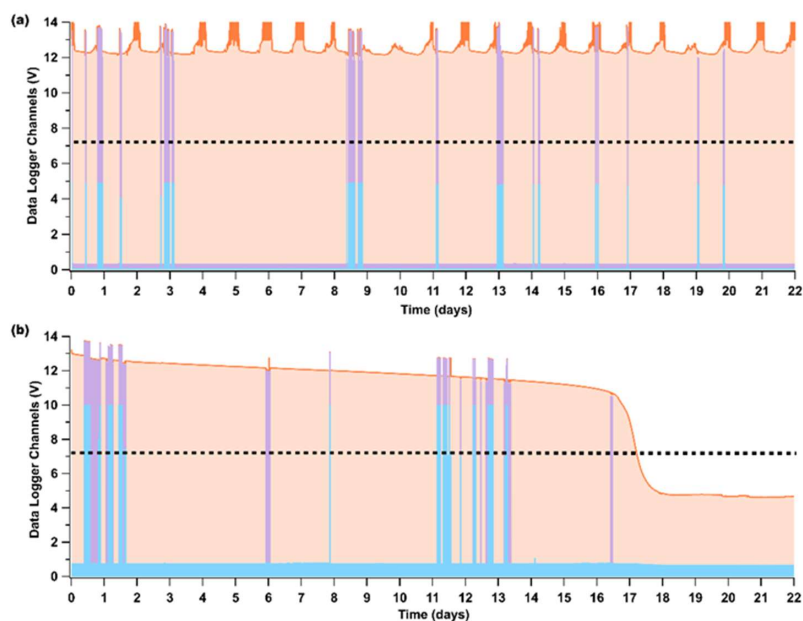
In comparison to two commercial samplers used by national monitoring networks, the power requirements of our new samplers are substantially lower. The first commercial sampler we reviewed draws a maximum of 2 A, with a ceramic heater housed within the sampler case that draws 0.8 A constantly, resulting in an upper limit power demand of 230 W (at 115 VAC) and a lower limit of 92 W. The commercial sampler can be upgraded to utilize a thermostated space heater for winter operation, drawing an additional 4.2 A (480 W), resulting in a maximum power demand of about 800 W when using a 115 VAC power supply. A second commercial precipitation sampler reviewed is used by national monitoring networks and draws approximately 5 A, resulting in a power requirement of 575 W at 115 VAC. The commercial and standard precipitation samplers for deposition monitoring programs have much higher power requirements compared to those presented in this work. The commercial samplers utilize 80 to 100 times more power. With our lower power requirements, the new automated samplers prove to be advantageous in both on- and off-grid sampling yet are disadvantaged in being unable to collect snow in the winter.

3.2.2 Precipitation Sampler Performance Tests and Data Logging

In addition to low power consumption during precipitation sampling, a supplied battery can obtain constant power renewal when outfitted with a solar top-up that is kept exposed to sunlight by proper orientation. At NL-BELT, adjustments were made for this during each site



612 visit during sample collection. During the solar top-up tests below, voltages of the sensor and
613 batteries were consistently monitored. Over a test period of 22 days, no appreciable decline in
614 battery performance of a 76 Ah unit was observed despite the detection of more than 10 rain
615 events during that period (Figure 3a).
616



617
618 **Figure 3.** Performance of off-grid precipitation samplers during sample collections from (a) 13
619 July to 7 August 2018, using a 76 Ah battery and solar panel top-up and (b) 22 January to 13
620 February 2019 with a 103 Ah battery and no solar panel. Battery voltage (shaded orange) is
621 elevated above 12 VDC when charging, or decreases over time when no solar panel is used and
622 precipitation is sensed/collected. The 12 VDC rain sensor relay signal (purple) and the open
623 sampling lid switch voltage (blue) indicate active periods of detected precipitation. The black
624 dashed line indicates the 60% efficiency cut off, 7.2 V, at which the battery should be recharged.
625

626 In comparison, winter sampling with these devices is not recommended without substantial
627 investment in a sufficient power density provided high-performance cold weather batteries. The
628 lack of sunlight during winter at higher latitudes also negates the use of effective small scale solar
629 top-up. Our tests show that when the samplers were deployed without a solar backup under snow-
630 free winter conditions (temperatures ranging from -17.8 to 7 °C), with a 103 Ah battery, the off-
631 grid system only lasted for 17 days. At this point, the larger capacity battery was fully depleted by
632 frequent snow and rainfall – probably due to the heated precipitation sensor requiring additional



633 energy to phase change snow and ice to water and then to evaporate that water. This depletion
634 occurred despite housing the battery in an insulated enclosure during the test. In addition, on days
635 6 and 16, the precipitation sensor relay was activated but the lid did not rotate to the open position
636 (Figure 3b, blue trace). This could have been because the precipitation event was not intense
637 enough for the lid to open fully and trigger the 5 V lid open switch or because of snow and ice
638 buildup around the lids resulting in them being unable to physically open. Overall, these samplers
639 may be possible to deploy during the winter if line power can be supplied. Such a deployment
640 would further necessitate that the sampling funnel be heated to render a liquid sample for collection
641 in the jugs in addition to the sensor chute to prevent snow and ice accumulation. A heated funnel
642 would also prevent snow or ice accumulation on top of the automated lids. Together, such power
643 hungry requirements for winter operation exceed simple off-grid use with a battery package that
644 is easily transported into and out of remote field sites.

645

646 **3.3 Comparison of Sample Collection Volumes**

647 The automated samplers were collocated with total deposition samplers and deployed
648 across the experimental forests of four NL-BELT regions during the 2015 and 2016 growing
649 seasons to observe deposition trends. In addition, we compare these observations to the long-term
650 climate normals reported by ECCC and estimated deposition at 1 km x 1 km resolution from the
651 DAYMET reanalysis model (Table 1). Three automated samplers were deployed in the open to
652 collect incident precipitation (OF) and another three under the experimental forest site canopy
653 (TF). The mean OF volumes of triplicate measurements from south to north were 1.42, 1.38, 1.31,
654 and 0.79 L, whereas the corresponding TF volumes were generally similar in magnitude at 0.96,
655 0.98, 1.02, and 1.13 L, for the 2015-16 sampling period (Figure 4). It is evident that the volume of
656 precipitation decreased as latitude increased for OF samples, whereas the opposite relationship
657 was observed in TF samplers, although the absolute volumes are more comparable in magnitude.
658 The total deposition volumes collected were as expected, decreasing from south to north in
659 agreement with the expectations from the long-term normals and comparable to the estimates from
660 the DAYMET model (Table 1), where the largest integrated volume of precipitation was collected
661 in the lowest latitude (GC) and a lower amount in the highest latitude (ER), with the intermediate
662 sites (HR and PB) having the lowest inputs overall during this observation period. Total annual
663 deposition volumes collected by our deployed samplers from south to north in 2015 were 39.5,



664 39.4, 31.9, and 17.5 L, while in 2016, they were 51.7, 37.8, 32.8, and 34.2 L. Total deposition
665 volume collected from HR was used for comparison to automated sample volumes collected at PB
666 in 2015, as they both share the same watershed. This approach had to be taken, as the HR site was
667 initially planned for full experimental use before becoming inaccessible in early 2015. The relative
668 error between the two sites for samples collected in 2016 was $\pm 15\%$ (24.6 L in PB and 32.2 L in
669 HR), comparable to the reproducibility we observe for replicates collected within a given site (see
670 below). The total deposition samplers were installed in HR in late 2014 and the automated samplers
671 were then set up at PB. Despite this, there is good agreement between the trends in predicted
672 deposition values by DAYMET with the measured values, although the absolute amounts from
673 these are systematically lower in all of our observations. Sufficiently continuous measurements
674 from ECCC stations nearby each site are challenging to obtain for the 2015-16 period. When
675 available with greater than 80% coverage, the ECCC datasets both agree and disagree with our
676 observations in GC and SR, respectively, suggesting that there is substantial deposition volume
677 heterogeneity at the scale of ~ 10 km in this region. In SR, the disagreement with our measurements
678 is identical to the DAYMET model which uses ECCC observations as input data, while at GC the
679 ECCC measurements are identical to ours (Table S3). Further, the discrepancy in the PB or ER
680 average annual precipitation volume between ECCC and those of this work and DAYMET are not
681 possible to interrogate due to the large quantity of data missing from the ECCC monitoring station
682 (35.22% in ER and 39.65% in HR/PB; Table S3). The DAYMET observations are representative
683 of a larger spatial scale, where our discrete samplers could be subject to heterogeneity in deposition
684 (e.g., orographic precipitation, driven by topography like steep slopes) or impacted by
685 meteorological conditions not captured by the model (e.g., undercatch driven by local winds). The
686 temporally-resolved volume comparisons at sampling interval timescales better-demonstrates
687 comparability, despite the systematic differences. The month-to-month relationships between
688 DAYMET (and ECCC) and our observations all showed strong correlations at all sites, with linear
689 regressions having R^2 of 0.72 at ER, and 0.99, 0.99, and 0.86 (N/A, 0.941, N/A, and 0.934,
690 respectively) when progressing through the more southerly sites (Table S3). The discrepancy
691 between DAYMET, ECCC, and our observations for total deposition were highest in the most
692 northerly site, where the experimental site was located on a steep slope, with only 43 % of the
693 predicted volume collected. At all of the sample collection sites on the island of Newfoundland, a
694 consistent difference was observed with 65 ± 4 % of the estimated volume collected, except at GC



695 where our measurements and those from ECCC are identical and starkly contrasting to DAYMET.
696 Overall, parsing these comparisons is difficult and demonstrates that there may be up to 55%
697 additional uncertainty in deposited species, should given measurements of a species be scaled for
698 a watershed like ER by concentration in total deposition samples. We propose, that by isolating
699 only the deposited analytes and using analyte fluxes instead of concentrations in precipitation
700 samples, that uncertainty issues in representing volumes, improves overall deposition budget
701 certainties. Regardless, by following the recommended siting criteria from the NADP and
702 CAPMoN as best as possible, the very strong agreement of our temporal trends at both annual and
703 monthly timescales with both comparators demonstrates the suitability of the total deposition
704 samplers and therefore the automated samplers for use in quantifying deposited chemical species
705 of atmospheric interest into the experimental sites.

706 The wet deposition volumes collected for the snow free period using the automated
707 precipitation samplers did not follow the trends in total deposition (Figure 4), as might be expected.
708 For the 2015 collection period from June through October, the summed volumes of OF
709 precipitation, from south to north across the NL-BELT, were 25.4, 10.9, 20.4, and 2.2 L, while in
710 2016 they were 17.3, 30.4, 13.5, and 5.1 L. There are three reasons as to why the measured wet
711 deposition volumes do not follow the total deposition trend across the transect. First, these
712 samplers are designed specifically to collect only conductive precipitation (i.e., containing
713 conductive atmospheric compounds) not total/bulk precipitation. As a result, the OF wet
714 deposition volume collected across the sites is mostly below 50% of total volumes collected, while
715 TF volumes are similar in magnitude or lower than that of OF (Figure 4). The wet deposition
716 fraction collected was variable within and between regions, sometimes less than 10%, despite large
717 volumes collected in total and presumably due to intense atmospheric washout that this region is
718 well-known for. Second, the NL-BELT total deposition trend estimated using the ECCC long-term
719 climate normals represents a 30-year period (Bowering et al., 2022) while the automated volume
720 measurements here represent two years of targeted conductive precipitation collection. The
721 combined summed volumes of targeted conductive wet deposition across the 2015 and 2016 field
722 seasons were 42.7, 41.3, 33.9, and 7.3 L, somewhat better reflect the expected precipitation trends
723 within the transect (Table 1). Lastly, our monthly automated wet deposition sample collection
724 periods occurred from June through November and so it is temporally incomplete with respect to
725 the substantial amount of precipitation volume deposited as snow delivered during the winter



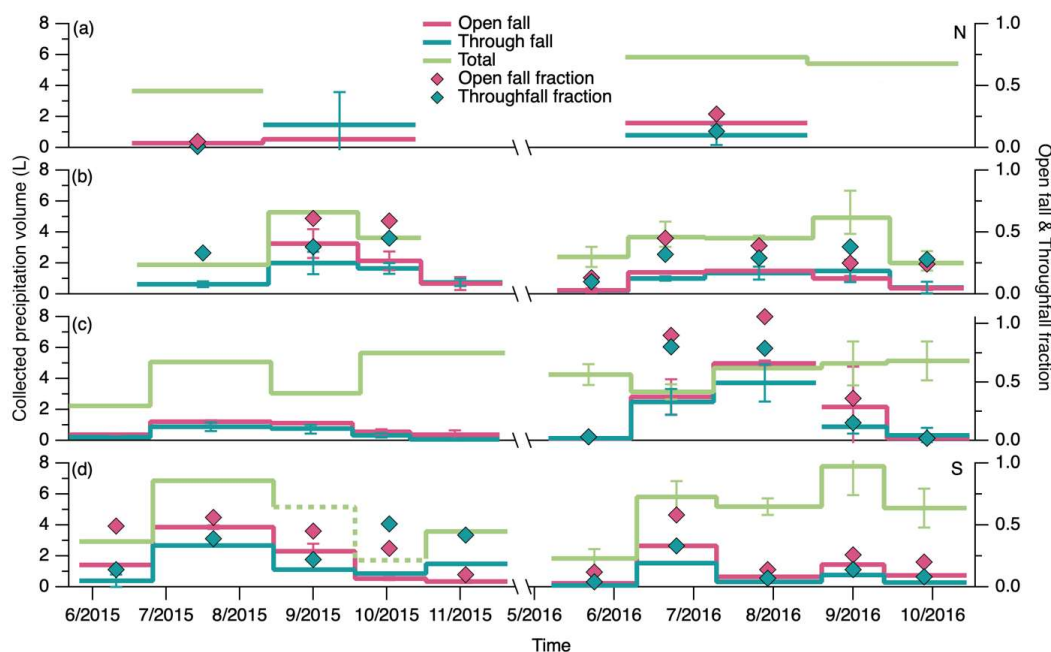
726 (Table S3). The discrepancies between the long-term trends and our shorter-term observations
727 therefore make sense as they are sensitive to interannual changes in synoptic scale transport and
728 rainwater solute loadings, as exemplified by the volumes collected in SR in 2015 (Figure 4b) and
729 PB in 2016 (Figure 4c). Overall, for the automated sampler observations on a per-year basis, there
730 is no consistent trend between site latitude and the volume collected in either OF or TF. This is
731 unsurprising as they are dependent on the conditions that drive the rate of atmospheric wash-out
732 and presence of conductive solutes.

733 The automated OF wet deposition volumes collected each year have peak values that range
734 from 1 to 4 L with an overall variability of $\pm 33\%$ for any triplicate of samples across the entire
735 dataset. Wind is known to generate bias in gauge-based precipitation measurements where
736 unshielded precipitation gauges can catch less than half of the amount of a shielded gauge (Colli
737 et al., 2016). A windscreens design for obtaining rainfall rates – and thus, volumes – to be more
738 reproducible could be considered in future deployments of our developed samplers, similar to
739 recently reported innovations for smaller rainfall rate devices (Kochendorfer et al., 2023). This
740 would however increase costs and logistical considerations in deploying the developed devices,
741 which currently operate synonymously to deposition systems employed by government monitoring
742 programs. In addition, collection of replicate samples allows our observations to span a wider
743 physical area, reducing the impact of confounding variables such as wind speed in comparison to
744 a more typical sample size of one for many field collections. Imperfect siting and lack of shielding
745 is necessary where remote field sampling prevents the setup of such infrastructure. Across our 33
746 sample collection periods, our replicate relative standard deviations (RSDs) follow a log-normal
747 distribution where volume reproducibility is typically within $\pm 12.5\%$ and almost always within \pm
748 31.5% (Figure S11). A few outliers with higher variability skew the overall view of volume
749 precision. Out of 33 OF samples collected, 8 have RSDs greater than 40.5% and 2 of those 8 have
750 RSDs greater than 100% . As a result, the deployment of triplicate samplers provides researchers
751 with a better opportunity to implement quality control as they can reduce bias in the event of
752 dynamic OF. While the effect of wind is reduced, additional factors can drive variability when the
753 samplers are placed under a forest canopy for TF collection.

754 To demonstrate canopy dynamics impacting interception volumes within the sampling
755 sites, the ratio of throughfall to open fall (TF/OF) volume was compared amongst our total pool
756 of 31 samples. This group of samples encompassed the monthly average TF/OF values for each



757 set of triplicate samplers, at all four sites, from 2015 to 2016. These measurements were then split
758 into two separate populations – samples that have a TF/OF less than one ($n=24$) and those that
759 have a TF/OF greater than one ($n=7$). The samplers were positioned identically between years and
760 no single sampler was reproducibly found in the second population. In the first population, the
761 fraction collected was $56 \pm 21\%$ (ranging from 19 to 88%), likely due to the known processes of
762 canopy and stem interception (Eaton et al., 1973; Howard et al., 2022). For example, in two young
763 balsam fir-white birch mixed forest stands, the amount of precipitation intercepted by the forest
764 canopy, in similar snow-free conditions, was estimated to be $11 \pm 5\%$ (Hadiwijaya et al., 2021).
765 In mature boreal forests, 9% to 55% of rainfall can be intercepted by the canopy (Pomeroy et al.,
766 1999). Relevant to deposition of atmospheric constituents, Pomeroy et al. (1999) also reported that
767 up to 70% of intercepted rainfall may evaporate directly from the canopy, which can leave behind
768 non-volatile rainfall solutes. Wet deposition that undergoes stemflow (SF) proceeds down the
769 branches, stems, and/or trunks of a plant, transferring precipitation and nutrients from the canopy
770 to the soil at the trunk or stem base (Ciruzzi and Loheide, 2021). These known mechanisms of
771 canopy interception ultimately reduce the amount of precipitation reaching the ground as TF, and
772 thus, the explain the smaller volumes found in our samplers compared to the OF measured
773 simultaneously. In contrast, the fractions that ranged from 108% to 424%, averaging 186%,
774 demonstrates a different aspect of the highly dynamic nature of canopies where they can sometimes
775 intercept rainfall like an impermeable surface to act as a funnel, guiding large volumes of
776 precipitation on to the ground, or in this case into the TF samplers (Metzger et al., 2019).



777
 778
 779
 780
 781
 782
 783
 784
 785
 786
 787
 788
 789
 790

Figure 4. Average volume collected from replicate automated samplers deployed from June 2015 to October 2016, from north (N) to south (S), at the NL-BELT field sites: **(a)** ER, **(b)** SR, **(c)** PB, and **(d)** GC. The red trace represents open fall, teal for throughfall, and light green for total deposition (the sum of conductive and non-conductive precipitation). The total precipitation volume depicted for PB, from July 2015 to November 2015, were collected at the nearby HR site in the same watershed since no total deposition measurements were in place at PB during this period. The missing volume for GC in 2015 was estimated from the determined ECCC station linear relationship and is presented as a broken line. The fraction of precipitation collected as open fall or throughfall, compared to the total deposition (right axis), are represented by diamonds of the corresponding color. Error bars represent the standard deviation of three measurements from replicate samples. The axis break spans the winter months when the off-grid automated samplers were stored.

791

3.4 Characterizing Chemical Parameters from NL-BELT

792
 793
 794
 795
 796
 797
 798

In addition to assessing physical parameters, chemical parameters were also evaluated in this work. Conductivity and pH are measurements commonly made on precipitation samples collected from the field and so incorporating them into our analysis is useful for instrumental validation. Additionally, with increasing recognition of their importance as a proxy for ROC estimation, and in biogeochemical carbon budget closure, DOC flux measurements were used to compare against a limited number of prior reports, each using different sampling or data interpretation strategies. These chemical measurements were also made in an underrepresented



799 part of the world in terms of atmospheric deposition sampling and are useful additions to the
800 overarching study of precipitation chemistry.

801

802 **3.4.1 Precipitation pH**

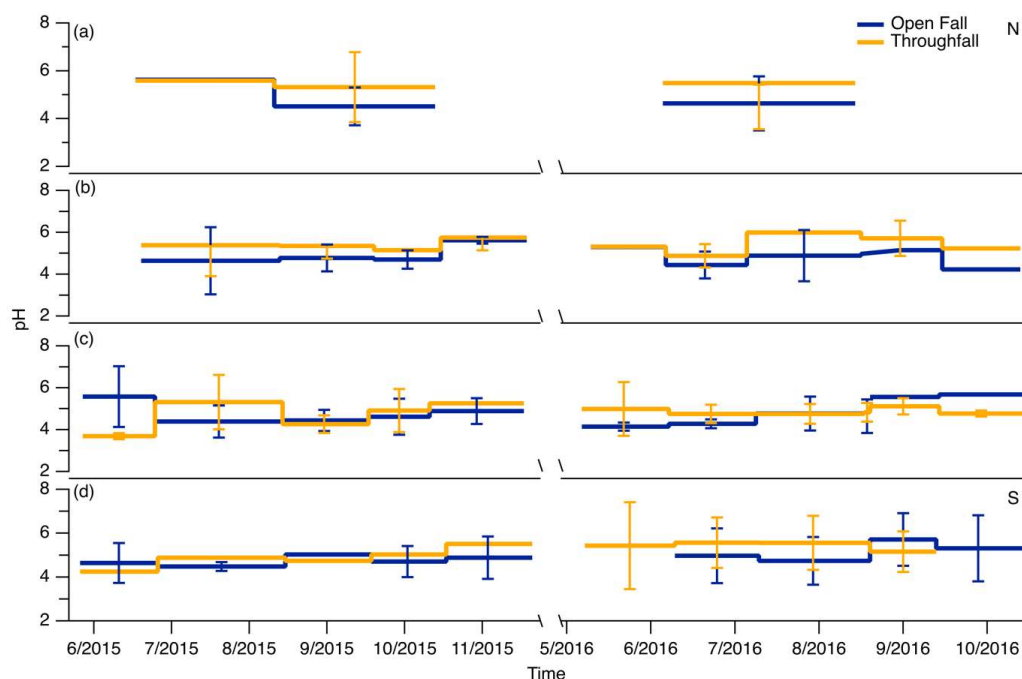
803 The deposition of atmospherically persistent pollutants and biogeochemically relevant species
804 to the Earth's surface, or even NO_3^- and SO_4^{2-} historically, can affect the environmental health of
805 soil, air, and water. With the pH range of natural rainwater in equilibrium with atmospheric CO_2
806 expected to be between 5.0 to 5.6, acid rain is defined by values lower than this (Han et al., 2019).
807 Traditionally, the extent of acidity depended on the intercepted atmospheric concentrations of
808 HNO_3 and H_2SO_4 . In any case, monitoring acidity and deposition is especially relevant in remote
809 regions, where major uncertainties and gaps in deposition measurements and global ion
810 concentrations exist (Escarré et al., 1999; Vet et al., 2014). A change in pH can modify the
811 chemical state of many pollutants, altering their transport, bioavailability, and solubility (Guinotte
812 and Fabry, 2008). For example, this can increase exposure and toxicity of metals and nutrients in
813 marine habitats which can go undetected for longer periods in remote areas.

814 Most TF samples were observed to have slightly higher pH (4.74 to 5.99) than those from OF
815 which had pH values ranging from 4.14 to 5.71 (Figure 5). The four remote NL-BELT sites are
816 dominated by balsam fir trees underlain by humo-ferric podzol soil with pH ranging between 3.0
817 and 4.5 (Table 1). In comparing the pH of podzolic soil to that of the collected TF, it was observed
818 that on average, the collected precipitation has a slightly more basic pH – with rare exceptions
819 (e.g., July and September 2015 PB pH of 3.69 and 4.26, respectively, and the July 2015 GC with
820 pH of 4.12). Excluding these exceptions, the TF precipitation pH ranged from 4.74 to 5.99 with
821 no major variations observed spatially between the four sites, or temporally between seasons or
822 years (Figure 5). The pH values reported at each of the NL-BELT field sites are comparable to
823 recent OF measurements made at CAPMoN sites in Nova Scotia and Newfoundland and Labrador,
824 where the reported pH of precipitation ranged from 4.44 to 5.19 (Houle et al., 2022).

825 Precipitation components have three possible fates upon entering soil, such that: i) acidic
826 components can be neutralized by free bases such as calcium carbonate (CaCO_3); ii) they can pass
827 into ground water; or iii) undergo exchange reactions with compounds already present on soil
828 surfaces. In particular, exchange of cations on negatively charged clay particles can occur and
829 impact soil properties, when exposed to acidic rainwater. This soil property is typically termed the



830 cation exchange capacity (CEC) and can impact the stabilization of organic matter (McFee et al.,
831 1977). There could be interactions between soil properties, like CEC, and precipitation
832 components, although this depends on the composition of the chemical system. At NL-BELT, the
833 CEC is lowest in the north at ER (7.8 cmol kg⁻¹) and highest in the next most northerly site at SR
834 (19.2 cmol kg⁻¹) and could be related to soil organic matter composition as well as the parent
835 material from which the mineral soil is derived (Patrick et al., 2022), in addition to its history
836 interacting with the ions delivered by incident rainfall. Upon interacting with precipitation, if the
837 water is acidic from the dissolution of strong acids like HNO₃ and H₂SO₄ to yield H₃O⁺,
838 undesirable cations such as Al³⁺ could be liberated from mineral soils, in addition to H₃O⁺
839 displacing beneficial nutrient cations for plants at exchanges sites throughout the soil, such as Mg²⁺
840 and Ca²⁺. However, in marine environments such as this, substantial amounts of dissolved cations
841 are also deposited (Feng et al., 2021) which act as spectator ions in aqueous solutions, having no
842 bearing on the measured acidity of precipitation. As a result, it is challenging to infer the extent to
843 which incident precipitation influences soil CEC at these sites without further experimental study.
844



845
846 **Figure 5.** Average pH values from replicate samples collected at each NL-BELT field site, from
847 north (N) to south (S), at (a) ER, (b) SR, (c) PB, and (d) GC, from June 2015 to August 2016.



848 Open fall collections are represented using the solid blue trace whereas the orange trace is the pH
849 of the precipitation collected as throughfall under the balsam fir canopy.

850
851 The more basic TF overall is expected, as it has been found that up to 90% of H_3O^+ in
852 precipitation can be absorbed by leaves while passing through the canopy (Cappellato et al., 1993).
853 Foliar leaching, the release of ions from leaves, has been commonly reported for base cations such
854 as Mg^{2+} , K^+ , and Ca^{2+} while being minimally observed for other ions such as Cl^- and SO_4^{2-} (Carlson
855 et al., 2003). Mechanisms for foliar leaching include passive cation exchange of H_3O^+ with, for
856 example, cells in the interior of the leaf (Burkhardt and Drechsel, 1997). Additionally, alkaline
857 dust – deposited on the leaves of the canopy, can decrease the acidity of TF precipitation. Such
858 dust can accumulate on leaf surfaces as a result of anthropogenic (i.e., industrial processes) or
859 natural (i.e., wind erosion) sources (Csavina et al., 2012), so that precipitation passing through the
860 canopy can interact with it (e.g., CaCO_3); thus, neutralizing acidic species and increasing the TF
861 pH observed in our automated samplers.

862 The pH of the collected precipitation appears to be similar in both TF and OF as a function of
863 time – despite the potential for foliar leaching and dust dissolution in the canopy. The same
864 chemical components may be setting the pH, as these measurements do not vary much seasonally,
865 geographically, or temporally. As pH is a long-studied measurement, its purpose in this work was
866 to validate the sample quality from our described collection approach, rather than drive any
867 scientific objective. Nevertheless, while the NL-BELT measurements demonstrate a recovery
868 compared to rainwater pH in 1980s eastern North America – prior to NO_x and SO_2 regulation (pH
869 from 4.1 to 5.0; Barrie and Hales, 1984), the present-day pH remains lower than expected for
870 natural rainwater (~5.6; Boyd, 2020). Keeping in mind the successful environmental policies
871 limiting SO_2 and NO_x , leading to considerable decreases in atmospheric concentrations of H_2SO_4
872 and HNO_3 , a modern view on the trajectory of continental U.S. cloud water composition and pH
873 has recently been reported (Lawrence et al., 2023). Across the U.S. and eastern Canada,
874 measurements of anion molar charge equivalents have been lower than cations – a potential
875 explanation being an increase in the presence of weak organic acids which commonly have pKa
876 values near 4 (Feng et al., 2021), an outcome we have also observed in aerosol sample chemical
877 composition from Atlantic Canada (Di Lorenzo et al., 2018). With the frequency of acid rain
878 having a pH < 5 decreasing over the past 20 years, these recently reported measurements depict
879 deposition composition shifting away from a ‘linear’ chemical regime dominated by H_3O^+ and



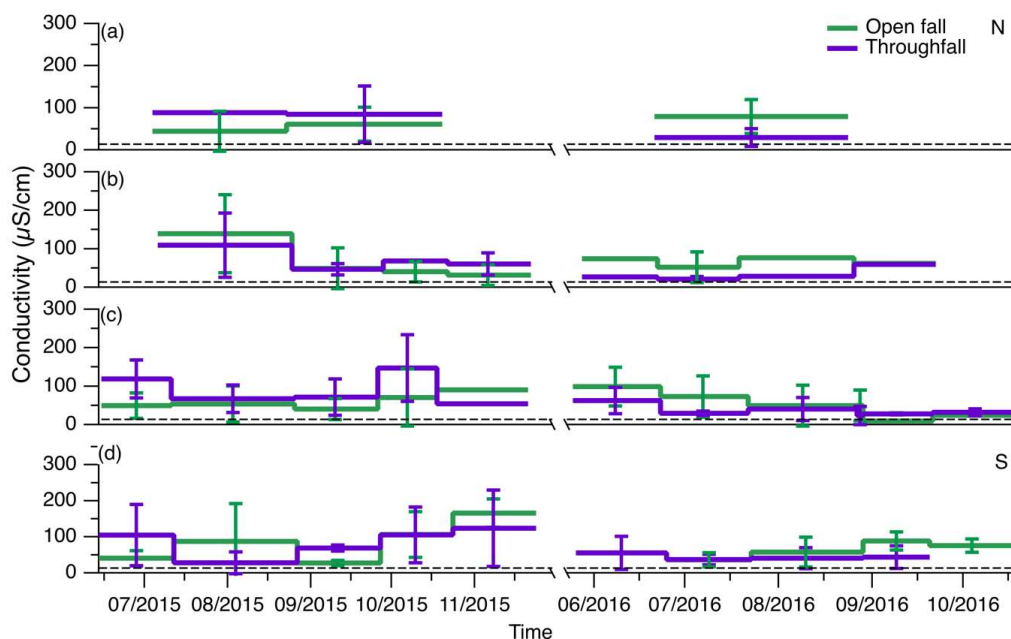
880 SO_4^{2-} towards a ‘non-linear’ regime designated by low acidity, moderate to high conductivity,
881 potentially weak acid-base buffer systems, and increasing base cation and TOC concentrations
882 (Lawrence et al., 2023). It would seem the evolving chemical contributors to global rainwater pH
883 remain an open line of investigation.

884

885 **3.4.2 Precipitation Conductivity**

886 In all the collected OF and TF precipitation samples, across all four NL-BELT sites, the
887 average measured conductivity values ranged from 21 to 166 $\mu\text{S}/\text{cm}$ (Figure 6). With the typical
888 conductivity of surface and drinking waters being between 1 to 1000 $\mu\text{S}/\text{cm}$ (Lin et al., 2017), and
889 typically below 200 $\mu\text{S}/\text{cm}$ in stream water measurements within the watersheds of each of the
890 NL-BELT sites, our observations are comparable and fall within the expected range. Our field
891 blanks – encompassing a variety of materials and apparatuses, and our cleaning procedures,
892 routinely produced conductivities of $9 \pm 5 \mu\text{S}/\text{cm}$. The conductivity of saturated HgCl_2 in water
893 (at 0.1% vol/vol) was $13.6 \pm 0.4 \mu\text{S}/\text{cm}$, which is also comparable to our field blanks and less than
894 what was observed for our samples. Even with this background correction applied, the conductivity
895 values presented here are expected to be similar to or higher than what would typically be found
896 in rainwater (4 to 150 $\mu\text{S}/\text{cm}$; Beverland et al., 1997) as the rain sensor deliberately selects for
897 precipitation containing ionic chemical components with conductivity greater than 1.0 $\mu\text{S}/\text{cm}$,
898 while excluding pure water during atmospheric washout, which would dilute the dissolved solutes
899 in the wet deposition sample and lower the resulting conductivity values. The overall
900 comparability between our range and those previously reported, where the lower limit is slightly
901 higher in our dataset, demonstrates that the principle of operation of our instrument is robust. It
902 decisively collects precipitation with the property of conductance indicating dissolved ionic solutes
903 of interest to atmospheric chemical processes.

904



905
906 **Figure 6.** Average conductivity measured from replicate automated samplers at the NL-BELT
907 field sites, from north (N) to south (S), at (a) ER, (b) SR, (c) PB, and (d) GC, from June 2015 to
908 October 2016. The green trace represents open fall samplers whereas the purple trace represents
909 throughfall samples. The error bar represents the standard deviation between replicate
910 measurements. The dashed black line represents the upper threshold of conductivity (13.6 $\mu\text{S}/\text{cm}$)
911 that arises due when an addition of saturated aqueous HgCl_2 is made to microbially sterilize
912 samples. Note that all samples have conductivities equivalent to or higher than 13.6 $\mu\text{S}/\text{cm}$.

913

914

3.4.3. Wet Deposition of Dissolved Organic Carbon (DOC) at NL-BELT

915

916

917

918

919

920

921

922

923

924

925

The concentration of DOC in OF and TF precipitation, across all four sites, ranged from 3 to 46 mg L^{-1} and 5 to 65 mg L^{-1} with averages of $16 \pm 10 \text{ mg L}^{-1}$ and $22 \pm 12 \text{ mg L}^{-1}$, respectively (Table 3). Concentrations are influenced by the volume collected and are not useful when discerning deposition trends and/or mechanisms. The concentrations were converted to elemental fluxes ($\text{mg C m}^{-2} \text{d}^{-1}$) using the volume of precipitation collected, the area of the funnel and the number of sampling days of each sampling period (Figure 7). The total flux for each sample period was summed to determine the annual flux and ranged from 600 to 4200 $\text{mg C m}^{-2} \text{a}^{-1}$ across the study sites for the snow free period (Table S4).

The TF DOC fluxes were enhanced compared to the corresponding OF samples as precipitation was intercepted by the forest canopy, with fluxes higher in TF samples by 600, 400, and 400 $\text{mg C m}^{-2} \text{a}^{-1}$ at GC, SR, and ER, respectively (Table S5). The accumulation of water-



926 soluble organics on forest canopies that increases DOC detected in TF could originate in part from
927 organic carbon-containing compounds aged through oxidation reactions in the atmosphere, which
928 increases their water solubility and propensity for surface interactions. In periods without
929 substantial rain, these oxidized organics deposit effectively to the high surface area of forest
930 canopies, contributing to the elevated DOC measured in TF. Additionally, non-volatile organics
931 left behind from evaporated precipitation intercepted by the canopy could also contribute.
932 Conversely, other mechanisms within the forest could result in enhanced DOC in TF. Recently,
933 Cha et al. (2023) utilized a mass balance approach to determine whether DOC deposition is driven
934 by canopy leaching (i.e., soluble tree resin, leaf exudates, internal tissues and microbes) or
935 dissolution of dry deposited gases and PM_{2.5} on plant foliage into rainwater. It was found that
936 canopy leaching is the major contributor to TF DOC, accounting for ~83% of throughfall DOC.
937 Whereas, PM_{2.5} and rainwater only accounted for ~3 and 14%, respectively, while dry deposited
938 gases were not considered. This suggest that internal cycling of DOC within the forest could an
939 important source of DOC to the throughfall soil interface (Cha et al., 2023). It is possible that a
940 similar mechanism may be responsible for the elevated levels of DOC in TF at the NL-BELT sites,
941 but we cannot explicitly distinguish between internal cycling versus external deposition in the
942 current study.

943 A notable exception was observed at PB, where the DOC fluxes in the open fall sample
944 was enhanced up to 1800 mg C m⁻² a⁻¹ when compared to the TF in 2016. This may be attributed
945 to a difference in forest type within this NL-BELT region being black spruce (*Picea mariana*)
946 instead of balsm fir (Bowering et al., 2023). Some studies have suggested that forest type could be
947 a major factor affecting DOC variability (Arisci et al., 2012; Sleutel et al., 2009). Specific
948 differences in canopy height, leaf area index, canopy structure and the shape of leaves and needles
949 could drive DOC differences between forest types (Smith, 1981; Erisman and Draaijers, 2003;
950 Sleutel et al., 2009). The elevated levels in OF samples relative to TF within PB are consistent
951 with idea of uptake and/or leaching of canopy DOC in the internal cycling of DOC, while the
952 enhanced TF at the rest of the sites is more difficult to observational constrain the participating
953 processes.

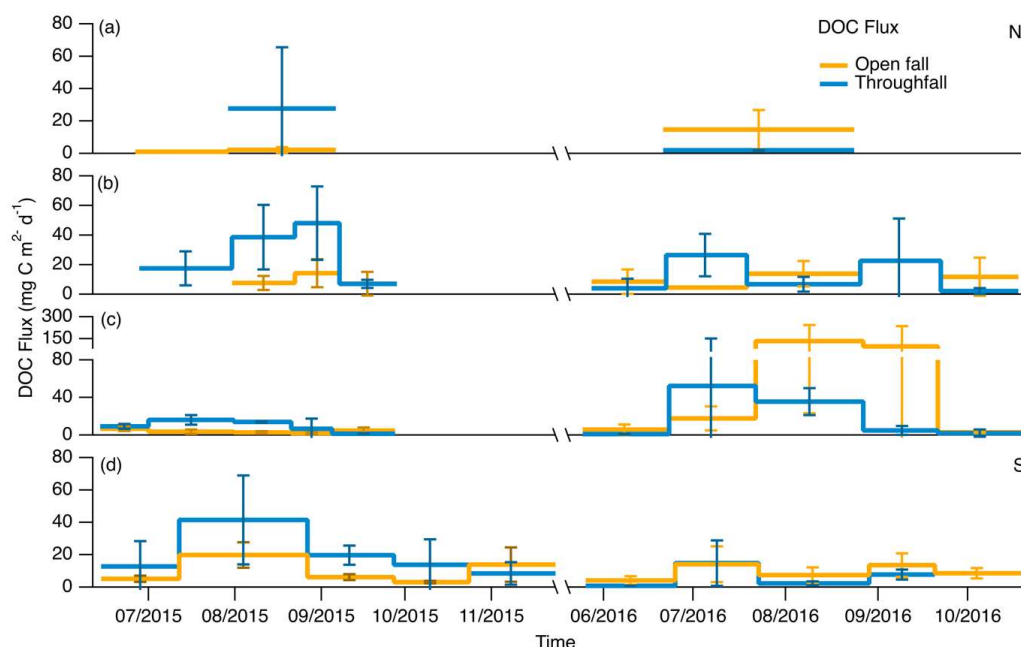
954 Episodic events, such as polluted air masses from wildfires could also result in elevated
955 deposition of DOC. It is estimated that ~116 – 385 Tg C a⁻¹ is produced globally due to the
956 incomplete combustion of biomass during landscape fires (Santín et al., 2016; Coward et al., 2022).



957 Several studies have associated enhanced DOC levels with wildfires (Gao et al., 2003; Moore,
958 2003; Wonaschütz et al., 2011; Myers-Pigg et al., 2015). More recently, Coward et al. (2022)
959 measured DOC in Pacific surface waters along the California coastline and observed 100 to 400
960 % increases in DOC concentration, when compared to pre-wildfire conditions. It is possible that a
961 similar biomass burning plume that underwent atmospheric washout, could be responsible for the
962 enhancement in the observed DOC at NL-BELT, overlaid on a background more typical of
963 seasonal oxidation of biogenic DOC. This also coincides with the seasonal variability observed in
964 OF samples from the same summer where elevated levels of DOC were measured. For instance,
965 the DOC deposition at PB for August 2016 was 4800 mg C m^{-2} , whereas the total deposition for
966 the same year was $7800 \text{ mg C m}^{-2} \text{ a}^{-1}$. This single period accounts for 62% of the total DOC
967 deposition at this site. This underscores the pivotal role that episodic transport may play in
968 influencing the dynamics of DOC deposition, particularly with a warming future where wildfires
969 are more prevalent.

970 The deposition trend observed in the current study also highlights the complexity of the
971 varied drivers of atmospheric ROC, in which some months have more DOC in TF versus OF and
972 occasionally the opposite is observed. Generally, we observed similar fluxes in both samples –
973 suggesting that the amount of deposited carbon is comparable. Although the volume of
974 precipitation captured in TF samplers are generally lower when compared to the corresponding
975 OF samplers, the deposition flux of DOC is greater in TF samplers. With DOC enhanced in TF
976 samples, the values reported here could be an underestimation of the amount of carbon reaching
977 the forest floor during precipitation events due to competing processes within the canopy. One
978 such process is stemflow (SF), where a fraction of precipitation intercepted by the forest canopy
979 is funneled over the bark of the tree surface to the base of the tree stem (Oka et al., 2021). Although,
980 SF was not measured in the current study, several studies have demonstrated that DOC
981 concentrations are enhanced in SF when compared to the corresponding TF and bulk precipitation
982 samples (Stubbins et al., 2017; Van Stan and Stubbins, 2018; Ryan et al., 2021). Additionally, we
983 cannot rule out that the chemical speciation differs between OF, TF, and SF even if the DOC values
984 are similar, but such insights require more selective instrumentation for chemical analysis (e.g.,
985 high resolution mass spectrometry).

986



987
988 **Figure 7.** Average DOC fluxes ($\text{mg C m}^{-2} \text{d}^{-1}$) in replicate samples collected at the NL-BELT field
989 sites, from north (N) to south (S), at (a) ER, (b) SR, (c) PB, and (d) GC, from June 2015 to August
990 2016. The yellow trace represents samplers that were placed in the open without any obstruction
991 whereas the blue trace represents samplers that were placed under the canopy. Error bars represent
992 the standard deviation of three measurements from three independent samples.

993

994

995

996 Mean annual DOC fluxes were generally similar to those reported in some other boreal
997 forests (Table 3). These include Finland, with work in stands that consisted mainly of Scots pine
998 (*Pinus sylvestris L.*) (mean OF 2.32; TF, 4.35 $\text{g C m}^{-2} \text{a}^{-1}$; Pumpanen et al., 2014), as well as in
999 Mont St. Hilarie, Québec (mean OF 0.49; TF 2.05 $\text{g C m}^{-2} \text{a}^{-1}$; Dalva and Moore, 1991), which also
1000 consisted of a variety of tree species such as yellow birch (*Betula allenghanien*), red maple (*Acer*
1001 *rubrum*), and sugar maple (*Acer saccharum*). Conversely, the annual fluxes were orders of
1002 magnitude lower than measurements made at the University of Georgia (23 to 48 $\text{g C m}^{-2} \text{a}^{-1}$) which
1003 has a subtropic climate consisting mainly of southern live oak (*Quercus virginiana Mill.*) and
1004 eastern red cedar (*Juniperus virginiana L.*) occasionally hosting dense epiphytes (Van Stan et al.,
1005 2017). This highlights the potential variability to expect when measuring DOC in different forest
1006 systems, as the annual DOC fluxes vary depending on factors such as climate, tree species
composition, and environmental conditions.



1007 These results underscore the pivotal role the off grid custom-built automated deposition
1008 samplers can play in advancing scientific research, particularly in precipitation monitoring and
1009 analysis. The automated system enabled long term continuous sample collection in remote
1010 locations, which was previously challenging to attain due to the need for frequent human
1011 intervention and resources required to regularly access these experimental forest stands. These
1012 samplers also allowed us to compare DOC through replicate measurements in TF and OF samples
1013 which sheds light on the potentially different DOC deposition chemistries within the NL-BELT
1014 region. The automated system better maintains the integrity of DOC in the samples, since the
1015 introduction of forest litter could result in a positive bias for DOC in the collected precipitation.
1016 The use of replicates also results in more robust scientific conclusions and broader applicability of
1017 the results, and they can be obtained for a fraction of the cost of a commercial equivalent,
1018 highlighting the contribution these automated systems are capable of when applied to current
1019 precipitation monitoring. As a result, these samplers show promise in the quantification of
1020 biogeochemical and anthropogenic chemical species of interest, which will be visited in future
1021 manuscripts drawing from the samples presented in this dataset, and others since obtained, but are
1022 beyond the scope of this manuscript in demonstrating the performance of this new instrumentation.

1023
1024
1025
1026
1027
1028
1029
1030
1031
1032
1033
1034

1035 **Table 3.** Concentrations (mg C L^{-1}) and annual fluxes ($\text{g C m}^{-2} \text{a}^{-1}$) of DOC in precipitation (P),
1036 open fall (OF), throughfall (TF), and stemflow (SF) collected at forested sites. Where volumes are
1037 not available for other studies, fluxes are not possible to calculate. The values reported in the
1038 current study are the estimated DOC flux for the wet deposition sampling period (~June through



1039 October) for each year and therefore represents the lower limit of DOC deposition, as the dataset
 1040 excludes snow.

Site	Type	Mean Concentration (mg C L ⁻¹)	Annual Flux (g C m ⁻² a ⁻¹)	References
Grand Codroy, NL, Canada (2015 to 2016)	OF	12.83	1.56	This study
	TF	23.40	2.20	
Pynn's Brook, NL, Canada (2015 to 2016)	OF	19.98	4.21	
	TF	21.24	2.44	
Salmon River, NL, Canada (2015 to 2016)	OF	16.14	1.33	
	TF	21.00	2.65	
Eagle River, NL, Canada (2015 to 2016)	OF	11.59	0.53	
	TF	28.26	0.86	
Mont St. Hilaire, QC, Canada (1987)	P	2.00	0.49	Dalva and Moore, 1991
	TF	12.13	2.05	
	SF	40.10	0.10	
Northern China (2007 to 2008)	P	2.4 to 3.9	1.4 to 2.7	Pan et al., 2010
Coulissenhieb, Northeast Bavaria (1995 to 1997)	P	2.70	-	Michalzik and Matzner, 1999
	TF	15.20	-	
Hobcaw Barony, South Carolina, USA (2014 to 2015)	P	1.20	-	Chen et al., 2019
	Pine TF	26.00	-	
	Oak TF	38.8	-	
University of Georgia, USA 2015 to 2016	TF Epiphyte Oak	17	23**	Van Stan et al., 2017
	TF Bare Cedar	20	32**	
	TF Epiphyte Cedar	54	48**	
SMEARII Site, Southern Finland (1998 to 2012)	P	3.24	2.32	Pumpanen et al., 2014
	TF	10.10	4.35	

** Estimated DOC yield for 2016 (g C m⁻² a⁻¹) where sampled storms values (g C event⁻¹) were scaled to an annual deposition value using meteorological data and a linear rainfall-DOC yield relationship.

1041 4 Conclusions

1042 This paper presents a cost-effective automated deposition sampler for continuous
 1043 collection of precipitation. An open-source procedure and schematics for building these samplers
 1044 is provided alongside the rationale for selecting the materials in the current study to target analytes
 1045 of scientific interest in wet deposition samples. These low-power systems are demonstrated in
 1046 being capable of continuous off-grid use for sample collection over two years at the NL-BELT
 1047 experimental sites, with replacement of battery power packs monthly or bimonthly, with on-grid



1048 performance also provided for comparison. The resulting systems enhance the accessibility of
1049 automated wet deposition samplers to scientists globally and this work highlights their robust
1050 performance in collecting and preserving rainwater conductivity and pH, alongside providing
1051 measurements of DOC from this understudied region that builds a broader picture of the
1052 atmosphere-surface exchange of this biogeochemical pool across the NL-BELT. Comparability
1053 and complementarity of our results to well-established and current measurements of interest like
1054 DOC, demonstrate their efficacy. The samples collected in this work from this new instrumentation
1055 are expected to be used further in several complementary and novel environmental monitoring
1056 studies in the future to extend our biogeochemical analysis, but also to study the transport of other
1057 anthropogenic pollutants of emerging interest, which are beyond the scope of describing our new
1058 platform. For the broader deposition-motivated community, the instrument design also allows for
1059 easy cost-effective modification of the number of replicate samplers, the material composition of
1060 all surfaces the aqueous samples interact with, as well as preservation strategies, depending on the
1061 analyte of interest. The capacity to autonomously collect wet deposition, in addition to traditional
1062 bulk deposition samples can shed light on competing wet and dry deposition processes. Should
1063 on-grid capacity suit scientific objectives, these samplers are anticipated to be possible for use
1064 year-round when paired with more power-intensive strategies to facilitate solid to liquid phase
1065 transfer for detected and collected precipitation in the winter.
1066
1067



1068 *Data availability.* The data are available from the corresponding author (TV) on request.

1069

1070 *Author contributions.* AC, DP, and ML performed the data analysis. AC and DP wrote the
1071 manuscript with contributions from all authors. Sampler design and construction were led by TV,
1072 with assistance from BP and RH for initial prototypes, DP and ML for the revised iteration, and
1073 AC for the final modular control boards. Sample collection and associated characterization
1074 measurements were performed by BP and TV. Conceptualization and conduct of the sampling
1075 experiments were made by TV, CY, KE, and SZ. All authors were involved in examining and
1076 reviewing the results. All authors were involved in editing the paper.

1077

1078 *Competing interests.* The contact author has declared that none of the authors has any competing
1079 interests.

1080

1081 **5 Acknowledgements**

1082 Funding for this work was provided by the Newfoundland and Labrador Department of
1083 Agrifoods and Forestry, Centre for Forestry Science and Innovation (Project 221269), and the
1084 Harris Centre at Memorial University. T. C. VandenBoer was supported for this work in-part
1085 through a Government of Canada Banting Postdoctoral Fellowship. Fieldwork sample collection
1086 by B. K. Place was supported by funding from Polar Knowledge Canada through the Northern
1087 Scientific Training Program. Additional financial support for full redesign of the samplers was
1088 provided through Environment and Climate Change Canada Grants & Contributions
1089 (GCXE20S009). A. A. Colussi acknowledges support for this work through a Natural Sciences
1090 and Engineering Research Council of Canada (NSERC) Graduate Scholarship – Master’s program
1091 (CGSM) and Ontario Graduate Scholarship (OGS). M. Lao acknowledges support for this work
1092 through a NSERC Undergraduate Student Research Award (USRA). We thank C. M. Laprise and
1093 C. Conlan for aid in the collection and organization of samples for analysis, supported in part by
1094 the Memorial University Career Experience Program (MUCEP) and V. Sitahai through a York
1095 University Dean’s Undergraduate Research Award (DURA). T. C. VandenBoer, C. J. Young and
1096 S. E. Ziegler were supported through the NSERC Discovery (RGPIN-2020-06166; RGPIN-2018-
1097 05990; RGPIN-2018-05383) and Strategic Partnerships (479224) Programs. The authors would
1098 also like to thank B. Hearn, D. Harris, A. Skinner, C. Young, J. J. MacInnis, J. Warren, and L.
1099 Souza for their invaluable assistance in sampling site access and set up, off-season storage of
1100 collection units, sample collection and analysis, and meteorological reanalysis. We thank H. Hung



1101 and C. Shunthirasingham for productive discussions on modular design and considerations for
1102 collection of persistent pollutants.

1103

1104 **6 References**

1105

1106 Altieri, K. E., Turpin, B. J., and Seitzinger, S. P.: Composition of Dissolved Organic Nitrogen in
1107 Continental Precipitation Investigated by Ultra-High Resolution FT-ICR Mass Spectrometry,
1108 *Environ. Sci. Technol.*, 43, 6950–6955, <https://doi.org/10.1021/es9007849>, 2009.

1109 Altieri, K. E., Hastings, M. G., Peters, A. J., and Sigman, D. M.: Molecular characterization of
1110 water soluble organic nitrogen in marine rainwater by ultra-high resolution electrospray ionization
1111 mass spectrometry, *Atmospheric Chem. Phys.*, 12, 3557–3571, <https://doi.org/10.5194/acp-12-3557-2012>, 2012.

1113 Amodio, M., Catino, S., Dambruoso, P. R., de Gennaro, G., Di Gilio, A., Giungato, P., Laiola, E.,
1114 Marzocca, A., Mazzone, A., Sardaro, A., and Tutino, M.: Atmospheric Deposition: Sampling
1115 Procedures, Analytical Methods, and Main Recent Findings from the Scientific Literature, *Adv.
1116 Meteorol.*, 2014, 161730, <https://doi.org/10.1155/2014/161730>, 2014.

1117 Arisci, S., Rogora, M., Marchetto, A., and Dichiaro, F.: The role of forest type in the variability of
1118 DOC in atmospheric deposition at forest plots in Italy, *Environ. Monit. Assess.*, 184, 3415–3425,
1119 <https://doi.org/10.1007/s10661-011-2196-2>, 2012.

1120 Barber, V. P. and Kroll, J. H.: Chemistry of Functionalized Reactive Organic Intermediates in the
1121 Earth's Atmosphere: Impact, Challenges, and Progress, *J. Phys. Chem. A*, 125, 10264–10279,
1122 <https://doi.org/10.1021/acs.jpca.1c08221>, 2021.

1123 Barrie, L. A. and Hales, J. M.: The spatial distributions of precipitation acidity and major ion wet
1124 deposition in North America during 1980, *Tellus B Chem. Phys. Meteorol.*, 36, 333–355,
1125 <https://doi.org/10.3402/tellusb.v36i5.14915>, 1984.

1126 Benedict, K. B., Day, D., Schwandner, F. M., Kreidenweis, S. M., Schichtel, B., Malm, W. C., and
1127 Collett, J. L.: Observations of atmospheric reactive nitrogen species in Rocky Mountain National
1128 Park and across northern Colorado, *Atmos. Environ.*, 64, 66–76,
1129 <https://doi.org/10.1016/j.atmosenv.2012.08.066>, 2013.

1130 Beverland, I. J., Heal, M. R., Crowther, J. M., and Srinivas, M. S. N.: Real-time measurement and
1131 interpretation of the conductivity and pH of precipitation samples, *Water. Air. Soil Pollut.*, 98,
1132 325–344, <https://doi.org/10.1007/BF02047042>, 1997.

1133 Bowering, K. L., Edwards, K. A., Wiersma, Y. F., Billings, S. A., Warren, J., Skinner, A., and
1134 Ziegler, S. E.: Dissolved Organic Carbon Mobilization Across a Climate Transect of Mesic Boreal
1135 Forests Is Explained by Air Temperature and Snowpack Duration, *Ecosystems*, 26, 55–71,
1136 <https://doi.org/10.1007/s10021-022-00741-0>, 2022.



- 1137 Bowering, K. L., Edwards, K. A., and Ziegler, S. E.: Seasonal controls override forest harvesting
1138 effects on the composition of dissolved organic matter mobilized from boreal forest soil organic
1139 horizons, *Biogeosciences*, 20, 2189–2206, <https://doi.org/10.5194/bg-20-2189-2023>, 2023.
- 1140 Boyd, C. E.: Carbon Dioxide, pH, and Alkalinity, in: *Water Quality: An Introduction*, edited by:
1141 Boyd, C. E., Springer International Publishing, Cham, 177–203, https://doi.org/10.1007/978-3-030-23335-8_9, 2020.
- 1143 Burkhardt, J. and Drechsel, P.: The synergism between SO₂ oxidation and manganese leaching on
1144 spruce needles — A chamber experiment, *Environ. Pollut.*, 95, 1–11,
1145 [https://doi.org/10.1016/S0269-7491\(96\)00126-1](https://doi.org/10.1016/S0269-7491(96)00126-1), 1997.
- 1146 Canadian Air and Precipitation Monitoring Network: Inspector’s Reference Manual -
1147 Precipitation, 1985.
- 1148 Cappellato, R., Peters, N. E., and Ragsdale, H. L.: Acidic atmospheric deposition and canopy
1149 interactions of adjacent deciduous and coniferous forests in the Georgia Piedmont, *Can. J. For.
1150 Res.*, 23, 1114–1124, <https://doi.org/10.1139/x93-142>, 1993.
- 1151 Carlson, J., Gough, W. A., Karagatzides, J. D., and Tsuji, L. J. S.: Canopy Interception of Acid
1152 Deposition in Southern Ontario, *Can. Field-Nat.*, 117, 523–530,
1153 <https://doi.org/10.22621/cfn.v117i4.799>, 2003.
- 1154 Casas-Ruiz, J. P., Bodmer, P., Bona, K. A., Butman, D., Couturier, M., Emilson, E. J. S., Finlay,
1155 K., Genet, H., Hayes, D., Karlsson, J., Paré, D., Peng, C., Striegl, R., Webb, J., Wei, X., Ziegler,
1156 S. E., and del Giorgio, P. A.: Integrating terrestrial and aquatic ecosystems to constrain estimates
1157 of land-atmosphere carbon exchange, *Nat. Commun.*, 14, 1571, <https://doi.org/10.1038/s41467-023-37232-2>, 2023.
- 1159 Cha, J.-Y., Lee, S.-C., Lee, E.-J., Lee, K., Lee, H., Kim, H. S., Ahn, J., and Oh, N.-H.: Canopy
1160 Leaching Rather than Desorption of PM_{2.5} From Leaves Is the Dominant Source of Throughfall
1161 Dissolved Organic Carbon in Forest, *Geophys. Res. Lett.*, 50, e2023GL103731,
1162 <https://doi.org/10.1029/2023GL103731>, 2023.
- 1163 Chen, H., Tsai, K.-P., Su, Q., Chow, A. T., and Wang, J.-J.: Throughfall Dissolved Organic Matter
1164 as a Terrestrial Disinfection Byproduct Precursor, *ACS Earth Space Chem.*, 3, 1603–1613,
1165 <https://doi.org/10.1021/acsearthspacechem.9b00088>, 2019.
- 1166 Chen, X., Xie, M., Hays, M. D., Edgerton, E., Schwede, D., and Walker, J. T.: Characterization of
1167 organic nitrogen in aerosols at a forest site in the southern Appalachian Mountains, *Atmospheric
1168 Chem. Phys.*, 18, 6829–6846, <https://doi.org/10.5194/acp-18-6829-2018>, 2018.
- 1169 Ciruzzi, D. M. and Loheide, S. P.: Monitoring Tree Sway as an Indicator of Interception Dynamics
1170 Before, During, and Following a Storm, *Geophys. Res. Lett.*, 48, e2021GL094980,
1171 <https://doi.org/10.1029/2021GL094980>, 2021.
- 1172 Clark, C. M., Phelan, J., Doraiswamy, P., Buckley, J., Cajka, J. C., Dennis, R. L., Lynch, J., Nolte,
1173 C. G., and Spero, T. L.: Atmospheric deposition and exceedances of critical loads from 1800–2025



- 1174 for the conterminous United States, *Ecol. Appl.*, 28, 978–1002, <https://doi.org/10.1002/eap.1703>,
1175 2018.
- 1176 Colli, M., Lanza, L. G., Rasmussen, R., and Thériault, J. M.: The Collection Efficiency of Shielded
1177 and Unshielded Precipitation Gauges. Part II: Modeling Particle Trajectories, *J. Hydrometeorol.*,
1178 17, 245–255, <https://doi.org/10.1175/JHM-D-15-0011.1>, 2016.
- 1179 Coward, E. K., Seech, K., Carter, M. L., Flick, R. E., and Grassian, V. H.: Of Sea and Smoke:
1180 Evidence of Marine Dissolved Organic Matter Deposition from 2020 Western United States
1181 Wildfires, *Environ. Sci. Technol. Lett.*, 9, 869–876, <https://doi.org/10.1021/acs.estlett.2c00383>,
1182 2022.
- 1183 Csavina, J., Field, J., Taylor, M. P., Gao, S., Landázuri, A., Betterton, E. A., and Sáez, A. E.: A
1184 review on the importance of metals and metalloids in atmospheric dust and aerosol from mining
1185 operations, *Sci. Total Environ.*, 433, 58–73, <https://doi.org/10.1016/j.scitotenv.2012.06.013>, 2012.
- 1186 Dalva, M. and Moore, T. R.: Sources and sinks of dissolved organic carbon in a forested swamp
1187 catchment, *Biogeochemistry*, 15, 1–19, <https://doi.org/10.1007/BF00002806>, 1991.
- 1188 Di Lorenzo, R. A., Place, B. K., VandenBoer, T. C., and Young, C. J.: Composition of Size-
1189 Resolved Aged Boreal Fire Aerosols: Brown Carbon, Biomass Burning Tracers, and Reduced
1190 Nitrogen, *ACS Earth Space Chem.*, 2, 278–285,
1191 <https://doi.org/10.1021/acsearthspacechem.7b00137>, 2018.
- 1192 Ditto, J. C., Joo, T., Slade, J. H., Shepson, P. B., Ng, N. L., and Gentner, D. R.: Nontargeted
1193 Tandem Mass Spectrometry Analysis Reveals Diversity and Variability in Aerosol Functional
1194 Groups across Multiple Sites, Seasons, and Times of Day, *Environ. Sci. Technol. Lett.*, 7, 60–69,
1195 <https://doi.org/10.1021/acs.estlett.9b00702>, 2020.
- 1196 Eaton, J. S., Likens, G. E., and Bormann, F. H.: Throughfall and Stemflow Chemistry in a Northern
1197 Hardwood Forest, *J. Ecol.*, 61, 495–508, <https://doi.org/10.2307/2259041>, 1973.
- 1198 Erisman, J. W. and Draaijers, G.: Deposition to forests in Europe: most important factors
1199 influencing dry deposition and models used for generalisation, *Environ. Pollut.*, 124, 379–388,
1200 [https://doi.org/10.1016/S0269-7491\(03\)00049-6](https://doi.org/10.1016/S0269-7491(03)00049-6), 2003.
- 1201 Escarré, A., Carratalá, A., Àvila, A., Bellot, J., Piñol, J., and Milán, M.: Precipitation Chemistry
1202 and Air Pollution, in: *Ecology of Mediterranean Evergreen Oak Forests*, edited by: Rodà, F.,
1203 Retana, J., Gracia, C. A., and Bellot, J., Springer Berlin Heidelberg, Berlin, Heidelberg, 195–208,
1204 https://doi.org/10.1007/978-3-642-58618-7_14, 1999.
- 1205 Farmer, D. K., Boedicker, E. K., and DeBolt, H. M.: Dry Deposition of Atmospheric Aerosols:
1206 Approaches, Observations, and Mechanisms, *Annu. Rev. Phys. Chem.*, 72, 375–397,
1207 <https://doi.org/10.1146/annurev-physchem-090519-034936>, 2021.
- 1208 Feng, J., Vet, R., Cole, A., Zhang, L., Cheng, I., O'Brien, J., and Macdonald, A.-M.: Inorganic
1209 chemical components in precipitation in the eastern U.S. and Eastern Canada during 1989–2016:
1210 Temporal and regional trends of wet concentration and wet deposition from the NADP and



- 1211 CAPMoN measurements, *Atmos. Environ.*, 254, 118367,
1212 <https://doi.org/10.1016/j.atmosenv.2021.118367>, 2021.
- 1213 Fingler, S., Tkalčević, B., Fröbe, Z., and Drevenkar, V.: Analysis of polychlorinated biphenyls,
1214 organochlorine pesticides and chlorophenols in rain and snow, *Analyst*, 119, 1135–1140,
1215 <https://doi.org/10.1039/AN9941901135>, 1994.
- 1216 Fowler, D.: Wet and Dry Deposition of Sulphur and Nitrogen Compounds from the Atmosphere,
1217 1980.
- 1218 Gao, S., Hegg, D. A., Hobbs, P. V., Kirchstetter, T. W., Magi, B. I., and Sadilek, M.: Water-soluble
1219 organic components in aerosols associated with savanna fires in southern Africa: Identification,
1220 evolution, and distribution, *J. Geophys. Res. Atmospheres*, 108,
1221 <https://doi.org/10.1029/2002JD002324>, 2003.
- 1222 Gregor, D. J. and Gummer, W. D.: Evidence of atmospheric transport and deposition of
1223 organochlorine pesticides and polychlorinated biphenyls in Canadian Arctic snow, *Environ. Sci.*
1224 *Technol.*, 23, 561–565, <https://doi.org/10.1021/es00063a008>, 1989.
- 1225 Grennfelt, P., Engleryd, A., Forsius, M., Hov, Ø., Rodhe, H., and Cowling, E.: Acid rain and air
1226 pollution: 50 years of progress in environmental science and policy, *Ambio*, 49, 849–864,
1227 <https://doi.org/10.1007/s13280-019-01244-4>, 2020.
- 1228 Guinotte, J. M. and Fabry, V. J.: Ocean Acidification and Its Potential Effects on Marine
1229 Ecosystems, *Ann. N. Y. Acad. Sci.*, 1134, 320–342, <https://doi.org/10.1196/annals.1439.013>,
1230 2008.
- 1231 Hadiwijaya, B., Isabelle, P.-E., Nadeau, D. F., and Pepin, S.: Observations of canopy storage
1232 capacity and wet canopy evaporation in a humid boreal forest, *Hydrol. Process.*, 35, e14021,
1233 <https://doi.org/10.1002/hyp.14021>, 2021.
- 1234 Hall, D. J.: Precipitation collector for use in the Secondary National Acid Deposition Network,
1235 United States, 1985.
- 1236 Han, G., Song, Z., Tang, Y., Wu, Q., and Wang, Z.: Ca and Sr isotope compositions of rainwater
1237 from Guiyang city, Southwest China: Implication for the sources of atmospheric aerosols and their
1238 seasonal variations, *Atmos. Environ.*, 214, 116854,
1239 <https://doi.org/10.1016/j.atmosenv.2019.116854>, 2019.
- 1240 Heald, C. L. and Kroll, J. H.: The fuel of atmospheric chemistry: Toward a complete description
1241 of reactive organic carbon, *Sci. Adv.*, 6, <https://doi.org/10.1126/sciadv.aay8967>, 2020.
- 1242 Heald, C. L., Gouw, J. de, Goldstein, A. H., Guenther, A. B., Hayes, P. L., Hu, W., Isaacman-
1243 VanWertz, G., Jimenez, J. L., Keutsch, F. N., Koss, A. R., Misztal, P. K., Rappenglück, B.,
1244 Roberts, J. M., Stevens, P. S., Washenfelder, R. A., Warneke, C., and Young, C. J.: Contrasting
1245 Reactive Organic Carbon Observations in the Southeast United States (SOAS) and Southern
1246 California (CalNex), *Environ. Sci. Technol.*, 54, 14923–14935,
1247 <https://doi.org/10.1021/acs.est.0c05027>, 2020.



- 1248 Houle, D., Augustin, F., and Couture, S.: Rapid improvement of lake acid–base status in Atlantic
1249 Canada following steep decline in precipitation acidity, *Can. J. Fish. Aquat. Sci.*, 79, 2126–2137,
1250 <https://doi.org/10.1139/cjfas-2021-0349>, 2022.
- 1251 Howard, M., Hathaway, J. M., Tirpak, R. A., Lisenbee, W. A., and Sims, S.: Quantifying urban
1252 tree canopy interception in the southeastern United States, *Urban For. Urban Green.*, 77, 127741,
1253 <https://doi.org/10.1016/j.ufug.2022.127741>, 2022.
- 1254 Iavorivska, L., Boyer, E. W., and DeWalle, D. R.: Atmospheric deposition of organic carbon via
1255 precipitation, *Acid Rain Its Environ. Eff. Recent Sci. Adv.*, 146, 153–163,
1256 <https://doi.org/10.1016/j.atmosenv.2016.06.006>, 2016.
- 1257 Jurado, E., Jaward, F. M., Lohmann, R., Jones, K. C., Simó, R., and Dachs, J.: Atmospheric Dry
1258 Deposition of Persistent Organic Pollutants to the Atlantic and Inferences for the Global Oceans,
1259 *Environ. Sci. Technol.*, 38, 5505–5513, <https://doi.org/10.1021/es049240v>, 2004.
- 1260 Jurado, E., Jaward, F., Lohmann, R., Jones, K. C., Simó, R., and Dachs, J.: Wet Deposition of
1261 Persistent Organic Pollutants to the Global Oceans, *Environ. Sci. Technol.*, 39, 2426–2435,
1262 <https://doi.org/10.1021/es048599g>, 2005.
- 1263 Kanakidou, M., Myriokefalitakis, S., Daskalakis, N., Fanourgakis, G., Nenes, A., Baker, A. R.,
1264 Tsigaridis, K., and Mihalopoulos, N.: Past, Present, and Future Atmospheric Nitrogen Deposition,
1265 *J. Atmospheric Sci.*, 73, 2039–2047, <https://doi.org/10.1175/JAS-D-15-0278.1>, 2016.
- 1266 Kochendorfer, J., Meyers, T. P., Hall, M. E., Landolt, S. D., and Diamond, H. J.: A new reference-
1267 quality precipitation gauge wind shield, *Atmospheric Meas. Tech. Discuss.*, 2023, 1–17,
1268 <https://doi.org/10.5194/amt-2023-2>, 2023.
- 1269 Kroll, J. H., Donahue, N. M., Jimenez, J. L., Kessler, S. H., Canagaratna, M. R., Wilson, K. R.,
1270 Altieri, K. E., Mazzoleni, L. R., Wozniak, A. S., Bluhm, H., Mysak, E. R., Smith, J. D., Kolb, C.
1271 E., and Worsnop, D. R.: Carbon oxidation state as a metric for describing the chemistry of
1272 atmospheric organic aerosol, *Nat. Chem.*, 3, 133–139, <https://doi.org/10.1038/nchem.948>, 2011.
- 1273 Kuylenstierna, J. C., Rodhe, H., Cinderby, S., and Hicks, K.: Acidification in developing countries:
1274 ecosystem sensitivity and the critical load approach on a global scale., *Ambio*, 30, 20–28,
1275 <https://doi.org/10.1579/0044-7447-30.1.20>, 2001.
- 1276 Lawrence, C. E., Casson, P., Brandt, R., Schwab, J. J., Dukett, J. E., Snyder, P., Yerger, E., Kelting,
1277 D., VandenBoer, T. C., and Lance, S.: Long-term monitoring of cloud water chemistry at
1278 Whiteface Mountain: the emergence of a new chemical regime, *Atmospheric Chem. Phys.*, 23,
1279 1619–1639, <https://doi.org/10.5194/acp-23-1619-2023>, 2023.
- 1280 Likens, G. E. and Butler, T. J.: Atmospheric Acid Deposition, in: *The Handbook of Natural*
1281 *Resources, Atmosphere and Climate*, vol. 6, edited by: Wang, Y., CRC Press, 2020.
- 1282 Lin, W.-C., Brondum, K., Monroe, C. W., and Burns, M. A.: Multifunctional Water Sensors for
1283 pH, ORP, and Conductivity Using Only Microfabricated Platinum Electrodes, *Sensors*, 17,
1284 <https://doi.org/10.3390/s17071655>, 2017.



- 1285 Lindberg, S. E., Lovett, G. M., Richter, D. D., and Johnson, D. W.: Atmospheric Deposition and
1286 Canopy Interactions of Major Ions in a Forest, *Science*, 231, 141–145,
1287 <https://doi.org/10.1126/science.231.4734.141>, 1986.
- 1288 Lovett, G. M.: Atmospheric Deposition of Nutrients and Pollutants in North America: An
1289 Ecological Perspective, *Ecol. Appl.*, 4, 629–650, <https://doi.org/10.2307/1941997>, 1994.
- 1290 Lovett, G. M. and Kinsman, J. D.: Atmospheric pollutant deposition to high-elevation ecosystems,
1291 *Atmospheric Environ. Part Gen. Top.*, 24, 2767–2786, [https://doi.org/10.1016/0960-](https://doi.org/10.1016/0960-1686(90)90164-I)
1292 [1686\(90\)90164-I](https://doi.org/10.1016/0960-1686(90)90164-I), 1990.
- 1293 McFee, W. W., Kelly, J. M., and Beck, R. H.: Acid precipitation effects on soil pH and base
1294 saturation of exchange sites, *Water. Air. Soil Pollut.*, 7, 401–408,
1295 <https://doi.org/10.1007/BF00284134>, 1977.
- 1296 Meteorological Service of Canada: 2004 Canadian Acid Deposition Science Assessment, , Library
1297 and Archives Canada, 2005.
- 1298 Metzger, J. C., Schumacher, J., Lange, M., and Hildebrandt, A.: Neighbourhood and stand
1299 structure affect stemflow generation in a heterogeneous deciduous temperate forest, *Hydrol. Earth*
1300 *Syst. Sci.*, 23, 4433–4452, <https://doi.org/10.5194/hess-23-4433-2019>, 2019.
- 1301 Michalzik, B. and Matzner, E.: Dynamics of dissolved organic nitrogen and carbon in a Central
1302 European Norway spruce ecosystem, *Eur. J. Soil Sci.*, 50, 579–590, [https://doi.org/10.1046/j.1365-](https://doi.org/10.1046/j.1365-2389.1999.00267.x)
1303 [2389.1999.00267.x](https://doi.org/10.1046/j.1365-2389.1999.00267.x), 1999.
- 1304 Midolo, G., Alkemade, R., Schipper, A. M., Benítez-López, A., Perring, M. P., and De Vries, W.:
1305 Impacts of nitrogen addition on plant species richness and abundance: A global meta-analysis,
1306 *Glob. Ecol. Biogeogr.*, 28, 398–413, <https://doi.org/10.1111/geb.12856>, 2019.
- 1307 Mohnen, V. A.: The Challenge of Acid Rain, *Sci. Am.*, 259, 30–39, 1988.
- 1308 Moore, T. R.: Dissolved organic carbon in a northern boreal landscape, *Glob. Biogeochem. Cycles*,
1309 17, <https://doi.org/10.1029/2003GB002050>, 2003.
- 1310 Myers-Pigg, A. N., Louchouart, P., Amon, R. M. W., Prokushkin, A., Pierce, K., and Rubtsov,
1311 A.: Labile pyrogenic dissolved organic carbon in major Siberian Arctic rivers: Implications for
1312 wildfire-stream metabolic linkages, *Geophys. Res. Lett.*, 42, 377–385,
1313 <https://doi.org/10.1002/2014GL062762>, 2015.
- 1314 National Atmospheric Deposition Program: NADP Site Selection and Installation Manual, 2009.
- 1315 Oka, A., Takahashi, J., Endoh, Y., and Seino, T.: Bark Effects on Stemflow Chemistry in a
1316 Japanese Temperate Forest I. The Role of Bark Surface Morphology, *Front. For. Glob. Change*, 4,
1317 <https://doi.org/10.3389/ffgc.2021.654375>, 2021.
- 1318 Pacyna, J. M.: Ecological Processes: Atmospheric Deposition, in: *Encyclopedia of Ecology*, vol.
1319 1, edited by: Jorgensen, S. E. and Fath, B. D., Elsevier Science, 275–285, 2008.



- 1320 Pan, Y., Wang, Y., Xin, J., Tang, G., Song, T., Wang, Y., Li, X., and Wu, F.: Study on dissolved
1321 organic carbon in precipitation in Northern China, *Atmos. Environ.*, 44, 2350–2357,
1322 <https://doi.org/10.1016/j.atmosenv.2010.03.033>, 2010.
- 1323 Patrick, M. E., Young, C. T., Zimmerman, A. R., and Ziegler, S. E.: Mineralogic controls are
1324 harbingers of hydrological controls on soil organic matter content in warmer boreal forests,
1325 *Geoderma*, 425, 116059, <https://doi.org/10.1016/j.geoderma.2022.116059>, 2022.
- 1326 Pekey, B., Karakaş, D., and Ayberk, S.: Atmospheric deposition of polycyclic aromatic
1327 hydrocarbons to Izmit Bay, Turkey, *Chemosphere*, 67, 537–547,
1328 <https://doi.org/10.1016/j.chemosphere.2006.09.054>, 2007.
- 1329 Pickard, H. M., Criscitiello, A. S., Spencer, C., Sharp, M. J., Muir, D. C. G., De Silva, A. O., and
1330 Young, C. J.: Continuous non-marine inputs of per- and polyfluoroalkyl substances to the High
1331 Arctic: a multi-decadal temporal record, *Atmospheric Chem. Phys.*, 18, 5045–5058,
1332 <https://doi.org/10.5194/acp-18-5045-2018>, 2018.
- 1333 Pomeroy, J. W., Granger, R., Pietroniro, J., Elliott, J., Toth, B., and Hedstrom, N.: Classification
1334 of the Boreal Forest for Hydrological Processes, in: Proceedings of the Ninth International Boreal
1335 Forest Research Association Conference, 1999.
- 1336 Pumpanen, J., Lindén, A., Miettinen, H., Kolari, P., Ilvesniemi, H., Mammarella, I., Hari, P.,
1337 Nikinmaa, E., Heinonsalo, J., Bäck, J., Ojala, A., Berninger, F., and Vesala, T.: Precipitation and
1338 net ecosystem exchange are the most important drivers of DOC flux in upland boreal catchments,
1339 *J. Geophys. Res. Biogeosciences*, 119, 1861–1878, <https://doi.org/10.1002/2014JG002705>, 2014.
- 1340 Richter, D. D. and Lindberg, S. E.: Wet Deposition Estimates from Long-Term Bulk and Event
1341 Wet-Only Samples of Incident Precipitation and Throughfall, *J. Environ. Qual.*, 17, 619–622,
1342 <https://doi.org/10.2134/jeq1988.00472425001700040017x>, 1988.
- 1343 Ryan, K. A., Adler, T., Chalmers, A., Perdrial, J., Shanley, J. B., and Stubbins, A.: Event Scale
1344 Relationships of DOC and TDN Fluxes in Throughfall and Stemflow Diverge From Stream
1345 Exports in a Forested Catchment, *J. Geophys. Res. Biogeosciences*, 126, e2021JG006281,
1346 <https://doi.org/10.1029/2021JG006281>, 2021.
- 1347 Safe, S.: Toxicology and Risk Assessment of POPs, in: Persistent Organic Pollutants, edited by:
1348 Fiedler, H., Springer Berlin Heidelberg, Berlin, Heidelberg, 223–235,
1349 https://doi.org/10.1007/10751132_8, 2003.
- 1350 Safieddine, S. A. and Heald, C. L.: A Global Assessment of Dissolved Organic Carbon in
1351 Precipitation, *Geophys. Res. Lett.*, 44, 11,672–11,681, <https://doi.org/10.1002/2017GL075270>,
1352 2017.
- 1353 Santín, C., Doerr, S. H., Kane, E. S., Masiello, C. A., Ohlson, M., de la Rosa, J. M., Preston, C.
1354 M., and Dittmar, T.: Towards a global assessment of pyrogenic carbon from vegetation fires, *Glob.
1355 Change Biol.*, 22, 76–91, <https://doi.org/10.1111/gcb.12985>, 2016.



- 1356 Sleutel, S., Vandenbruwane, J., De Schrijver, A., Wuyts, K., Moeskops, B., Verheyen, K., and De
1357 Neve, S.: Patterns of dissolved organic carbon and nitrogen fluxes in deciduous and coniferous
1358 forests under historic high nitrogen deposition, *Biogeosciences*, 6, 2743–2758,
1359 <https://doi.org/10.5194/bg-6-2743-2009>, 2009.
- 1360 Smith, W. H.: *Air Pollution and Forests: Interactions Between Air Contaminants and Forest*
1361 *Ecosystems*, 1st ed., Springer, New York, NY, 379 pp., 1981.
- 1362 Stedman, J. R., Heyes, C. J., and Irwin, J. G.: A comparison of bulk and wet-only precipitation
1363 collectors at rural sites in the United Kingdom, *Water, Air, Soil Pollut.*, 52, 377–395,
1364 <https://doi.org/10.1007/BF00229445>, 1990.
- 1365 Stoddard, J. L., Jeffries, D. S., Lükewille, A., Clair, T. A., Dillon, P. J., Driscoll, C. T., Forsius,
1366 M., Johannessen, M., Kahl, J. S., Kellogg, J. H., Kemp, A., Mannio, J., Monteith, D. T., Murdoch,
1367 P. S., Patrick, S., Rebsdorf, A., Skjelkvåle, B. L., Stainton, M. P., Traaen, T., van Dam, H.,
1368 Webster, K. E., Wieting, J., and Wilander, A.: Regional trends in aquatic recovery from
1369 acidification in North America and Europe, *Nature*, 401, 575–578, <https://doi.org/10.1038/44114>,
1370 1999.
- 1371 Stubbins, A., Silva, L. M., Dittmar, T., and Van Stan, J. T.: Molecular and Optical Properties of
1372 Tree-Derived Dissolved Organic Matter in Throughfall and Stemflow from Live Oaks and Eastern
1373 Red Cedar, *Front. Earth Sci.*, 5, <https://doi.org/10.3389/feart.2017.00022>, 2017.
- 1374 Thornton, M. M., Shrestha, R., Wei, Y., Thornton, P. E., Kao, S.-C., and Wilson, B. E.: Daymet:
1375 Monthly Climate Summaries on a 1-km Grid for North America, Version 4 R1,
1376 <https://doi.org/10.3334/ORNLDAAAC/2131>, 2022.
- 1377 Thornton, P. E., Running, S. W., and White, M. A.: Generating surfaces of daily meteorological
1378 variables over large regions of complex terrain, *Aggreg. Descr. Land-Atmosphere Interact.*, 190,
1379 214–251, [https://doi.org/10.1016/S0022-1694\(96\)03128-9](https://doi.org/10.1016/S0022-1694(96)03128-9), 1997.
- 1380 Thornton, P. E., Shrestha, R., Thornton, M., Kao, S.-C., Wei, Y., and Wilson, B. E.: Gridded daily
1381 weather data for North America with comprehensive uncertainty quantification, *Sci. Data*, 8, 190,
1382 <https://doi.org/10.1038/s41597-021-00973-0>, 2021.
- 1383 United States Environmental Protection Agency: Integrated Science Assessment (ISA) for Oxides
1384 of Nitrogen, Oxides of Sulfur and Particulate Matter Ecological Criteria (Final Report, 2020), U.S.
1385 Environmental Protection Agency, Washington, DC, 2020.
- 1386 Van den Berg, M., Birnbaum, L. S., Denison, M., De Vito, M., Farland, W., Feeley, M., Fiedler,
1387 H., Hakansson, H., Hanberg, A., Haws, L., Rose, M., Safe, S., Schrenk, D., Tohyama, C., Tritscher,
1388 A., Tuomisto, J., Tysklind, M., Walker, N., and Peterson, R. E.: The 2005 World Health
1389 Organization Reevaluation of Human and Mammalian Toxic Equivalency Factors for Dioxins and
1390 Dioxin-Like Compounds, *Toxicol. Sci.*, 93, 223–241, <https://doi.org/10.1093/toxsci/kf1055>, 2006.
- 1391 Van Stan, J. T. and Stubbins, A.: Tree-DOM: Dissolved organic matter in throughfall and
1392 stemflow, *Limnol. Oceanogr. Lett.*, 3, 199–214, <https://doi.org/10.1002/lol2.10059>, 2018.



- 1393 Van Stan, J. T., Wagner, S., Guillemette, F., Whitetree, A., Lewis, J., Silva, L., and Stubbins, A.:
1394 Temporal Dynamics in the Concentration, Flux, and Optical Properties of Tree-Derived Dissolved
1395 Organic Matter in an Epiphyte-Laden Oak-Cedar Forest, *J. Geophys. Res. Biogeosciences*, 122,
1396 2982–2997, <https://doi.org/10.1002/2017JG004111>, 2017.
- 1397 VandenBoer, T. C.: AIM-IC: Applications to Nitrous Acid (HONO) in the Ambient Atmosphere
1398 and Precipitation Monitoring, Masters of Science, University of Toronto, 2009.
- 1399 Vet, R., Artz, R. S., Carou, S., Shaw, M., Ro, C.-U., Aas, W., Baker, A., Bowersox, V. C.,
1400 Dentener, F., Galy-Lacaux, C., Hou, A., Pienaar, J. J., Gillett, R., Forti, M. C., Gromov, S., Hara,
1401 H., Khodzher, T., Mahowald, N. M., Nickovic, S., Rao, P. S. P., and Reid, N. W.: A global
1402 assessment of precipitation chemistry and deposition of sulfur, nitrogen, sea salt, base cations,
1403 organic acids, acidity and pH, and phosphorus, *Glob. Assess. Precip. Chem. Depos. Sulfur*
1404 *Nitrogen Sea Salt Base Cations Org. Acids Acidity PH Phosphorus*, 93, 3–100,
1405 <https://doi.org/10.1016/j.atmosenv.2013.10.060>, 2014.
- 1406 Wonaschütz, A., Hersey, S. P., Sorooshian, A., Craven, J. S., Metcalf, A. R., Flagan, R. C., and
1407 Seinfeld, J. H.: Impact of a large wildfire on water-soluble organic aerosol in a major urban area:
1408 the 2009 Station Fire in Los Angeles County, *Atmospheric Chem. Phys.*, 11, 8257–8270,
1409 <https://doi.org/10.5194/acp-11-8257-2011>, 2011.
- 1410 Zhu, X., Zhang, W., Chen, H., and Mo, J.: Impacts of nitrogen deposition on soil nitrogen cycle in
1411 forest ecosystems: A review, *Acta Ecol. Sin.*, 35, 35–43,
1412 <https://doi.org/10.1016/j.chnaes.2015.04.004>, 2015.
- 1413 Ziegler, S. E., Benner, R., Billings, S. A., Edwards, K. A., Philben, M., Zhu, X., and Laganière, J.:
1414 Climate Warming Can Accelerate Carbon Fluxes without Changing Soil Carbon Stocks, *Front.*
1415 *Earth Sci.*, 5, <https://doi.org/10.3389/feart.2017.00002>, 2017.
- 1416